An Overview of Radar and Its Role in Baseball and Golf

By Noa Nishizawa

Faculty Advisor: Robert A. Norwood

A Master's Report Submitted to the Faculty of the

WYANT COLLEGE OF OPTICAL SCIENCES

In Partial Fulfillment of the Requirements for the Degree of

Master of Science

In the Graduate College

THE UNIVERSITY OF ARIZONA

2023

TABLE OF CONTENTS

TABLE OF FIGURES **3**
ABSTRACT **4**
RADAR **5**
INTRODUCTION 5
WAVE PROPAGATION 7
RADAR ELEMENTS 9
OPERATING FUNDAMENTALS 11
MATHEMATICAL DESCRIPTION 18
REFERENCES 23
MICRO-DOPPLER **24**
SIGNATURES 25
CHALLENGES AND PERSPECTIVES 28
THEORY 29
MICRO MOTION 32
REFERENCES 38
TRACKMAN **40**
OVERVIEW 40
PGA TOUR 41
SCIENCE 42
IMPACT POSITION 45
TRAINING FEATURES 48
REFERENCES 52
MLB STATCAST **53**
OVERVIEW 53
SPIN RATE 56
LAUNCH ANGLE 61
REFERENCES 66
CONCLUSION **69**

TABLE OF FIGURES

Figure 1. Simple radar block diagram....9
Figure 2. Typical envelope of radar receiver....12
Figure 3. Transmitted and received pulse....13
Figure 4. Transmitted and received waveforms of Doppler shift....15
Figure 5. Target position in spherical coordinates....17
Figure 6. Received signal versus range....22
Figure 7. Micro-Doppler signature of helicopter rotor blades....26
Figure 8. Micro-Doppler signature of helicopter tail and rotor blades....26
Figure 9. Seventeen joint human model....27
Figure 10. Space and body fixed coordinate system describing object motion....30
Figure 11. Roll-pitch-yaw convention....32
Figure 12. Geometry of radar and object with translation and rotation....34
Figure 13. Geometry of radar and rotating object....36
Figure 14. Trackman normalization across ranging environmental conditions....43
Figure 15. Normalization options including environment and ball type....44
Figure 16. Trackman spectrogram of hit golf ball....45
Figure 17. Trackman spectrogram at impact and synced swing path images....46
Figure 18. Trackman visualization of impact position....47
Figure 19. Trackman spectrogram at impact with distinct spin sidebands....48
Figure 20. Launch direction requirements for making putt on a flat green....49
Figure 21. Club path and face angle overlay....50
Figure 22. Visualization of launch direction, putt break, and straight line to the hole....51
Figure 23. General MLB Statcast ballpark architecture....53
Figure 24. Average fastball spin rate from 2015-2021....57
Figure 25. Trevor Bauer tweet regarding spin rate controversy....58
Figure 26. Scoring value of batted balls in 2015 based on launch angle and exit velocity....62
Figure 27. Total home runs in a season from 1970-2016....64

ABSTRACT

This report presents an overview of how radar makes use of electromagnetic energy to detect the position and velocity of objects by sensing the frequency change induced by the Doppler effect. The micro-Doppler effect is also discussed as it is analyzed to identify the motion of an object's individual elements. The application of radar in Trackman golf systems and MLB Statcast have had considerable effects on how sports are played and consumed. Trackman utilizes a combination of Doppler radar and optical imaging to gather club and ball data such as ball flight and impact location. Trackman systems are in use by the PGA Tour, club manufacturers, instructors, and players of all levels. MLB Statcast was implemented in 2015 and utilizes similar technology to track ball and player movement. Statcast data insights such as spin rate and launch angle have led to several new rule changes as well as a new hitting philosophy that has taken over the sport.

RADAR

INTRODUCTION

Radar stands for **RA**dio **D**etection **A**nd **R**anging and is a technology that uses electromagnetic waves to detect and locate objects. The technology has revolutionized several industries including aviation, weather forecasting, military, and sports. Its origins can be traced to the late 1800s when Heinrich Hertz discovered radio waves and demonstrated that they could be both transmitted and received through air.[1]

The first practical radar system was invented in Christian Hulsmeyer in 1904 for the purpose of detecting the presence of ships in dense fog. It took until the 1930s and the threat of aerial warfare for serious interest in radar to begin. Sir Robert Watson-Watt led a team at the Radio Research Station in the UK to create the first working radar system on a Royal Navy ship, which was a critical development that assisted the British defend Germany in the Battle of Britain. Radar continued to play a vital role in warfare as it became an important technology in World War II for air defense, navigation, target acquisition, and bombing.[2]

After World War II, radar became more common in civilian applications as the first commercial radar system was installed at an airport in 1945 to assist with air traffic control. Weather radar was developed in the 1950s to detect precipitation and monitor weather patterns. Doppler technology was developed in the 1960s and 1970s, which allowed for the measurement of velocity and motion. In the following two decades,

synthetic aperture radar (SAR) technology was developed for high resolution imaging from space.[3]

Digital signal processing in the 21st century has led to more sophisticated radar systems that include phased array radar and radar networks. Radar has become an even more valuable tool as its technology has seen a significant increase in accuracy, resolution, and range capabilities. Another recent advancement is cognitive radar, which uses artificial intelligence to adapt radar parameters in real time. Millimeter-wave radar is also a newer technology that utilizes higher frequencies for higher resolution and the ability to see through certain materials.[3]

WAVE PROPAGATION

Radar emitted waves consist of both an electric (E) and magnetic (H) force field that propagate in free space at the speed of light. Interactions with matter along its path induce effects such as scattering, diffraction, and refraction in the same manner as visible light.[4] An antenna system focuses electromagnetic waves into beams characterized by sinusoidal spatial and temporal frequencies. The distance or time between successive wave peaks defines the wavelength λ. Frequency and wavelength are related to the speed of light by the equation:

$$c = \lambda f = 3 \times 10^8 \text{ m/s.} \qquad (1)$$

The microwave wavelength range is between 10^{-3} and 10^{-1} m and the microwave band resides in the upper end of the frequency spectrum and is most commonly used for radar purposes.

The electric field wave from a transmitting antenna at sufficient distance has time t and range r dependence given by

$$E(r, \theta, \phi, t) = (A(\theta, \phi))/r \ * \ cos[2\pi f(t - \tfrac{r}{c}) + \psi] \text{ V/m} \qquad (2)$$

where amplitude A is dependent on the direction of r from the radiation source and ψ is typically an unknown but constant phase. The vectors $\overline{E}$ and $\overline{H}$ are always perpendicular to when $|\overline{r}|$ is large compared to antenna dimensions. The electric field can be represented by a two-dimensional phasor diagram to depict the time and space dependence of amplitude and phase within an integral multiple of 2π. The principal factors characterizing a periodic electric field are amplitude $A(\theta, \phi)/r$ and phase

$2\pi f(t - \frac{r}{c}) + \psi$ so the electric field can be expressed as

$$E = \frac{A(\theta,\phi)}{r} exp[j2\pi f(t - \frac{r}{c}) + j\psi \qquad (3)$$

The time-averaged power density, or the average power over a period f^{-1}, $S(r, \theta, \phi)$ is represented as

$$S(r, \theta, \phi) = \frac{1}{2}\frac{EE^*}{\eta_0} = \frac{A^2(\theta.\phi)}{2\eta_0 r^2} \text{ Wm^-2} \qquad (4)$$

where * denotes complex conjugation and η_0 is the wave impedance in space and is the electric to magnetic field amplitude ratio. The time average is of significance because it represents the outward flow of energy from the source, which can be continuous or pulsed. The products of S and areas represent the power that is received, absorbed, and scattered by objects of interest.

The spatial resolution or discrimination between adjacent objects is dependent on wavelength, antenna size, and the first null in a circular diffraction pattern is approximated by

$$\Delta\theta = 140\lambda/D \text{ deg} \quad (5)$$

where D is the diameter of the antenna system. To obtain the real time and space dependence, the real part of any phasor must be taken and this is a principle element of Doppler radar.

RADAR ELEMENTS

Radar operates by transmitting electromagnetic energy and detecting the returned echo for target information such as position, range, reflectivity signature, and velocity.

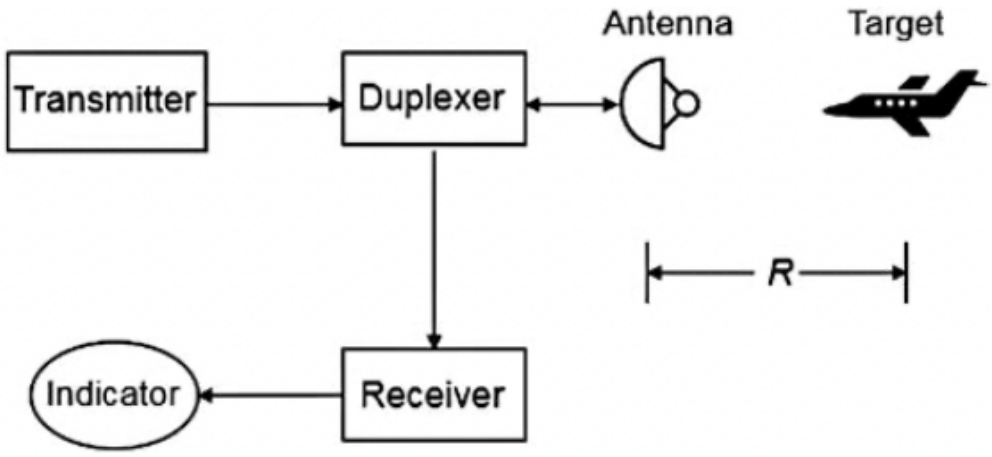

Figure 1. Simple radar block diagram[5]

An elementary radar system consists of a transmitter routing electromagnetic energy to the antenna via a duplexer or microwave device that allows the antenna to both transmit and receive energy. Tha antenna acts as a transducer to couple electromagnetic energy into free space at the speed of light and a small amount of the energy is reflected by the object and intercepted by the antenna at a time delay from transmission and reception at a range R by the relationship

$$t_d = 2R/c. \quad (6)$$

A functional pulse radar consists of five basic elements: a transmitter, a duplexer, an antenna, a receiver, and an indicator.[5]

The transmitter generates the radio frequency signal, continuous wave or pulsed, by either the power oscillator approach or master oscillator approach. The power oscillator approach generates a signal at the required level for direct application to the antenna and the master oscillator approach generates a low-power signal that is then amplified to the appropriate level.

The duplexer allows the antenna of monostatic radars to both transmit and receive since it consists of two gas discharge devices: transmit-receive (TR) and anti-transmit-receive (ATR). The transmit-receive device protects the receiver from high-power radar signal during transmission and the anti-transmit-receive directs the echo signal to the receiver.

Antennas in radar systems are typically highly directional such as a parabolic dish antenna fed from a feed antenna at its focus. The antenna focuses on concentrating the transmitted signal into a narrow beam in a preferred direction and then intercepting the target echo signal from that same direction.[6]

The receiver consists of a low noise radio frequency amplifier, a mixer, an intermediate frequency amplifier, a video amplifier, and a display unit. The front-end RF amplifier is usually a parametric amplifier or low-noise transistor and the mixer and local oscillator convert the RF signal into an IF signal. The intermediate frequency amplifier is designed as a match filter and the pulse modulation is extracted by a second detector then

amplified by the video amplifier, usually a cathode-ray tube (CRT), to a level suitable for indicator display.

The direction of the backscattered wavefront provides angular position information. When there is relative motion between the radar and the target, there is a shift in the carrier frequency of the reflected wave that is a measure of relative velocity known as the Doppler shift.

OPERATING FUNDAMENTALS

The target signal that is received by the radar is often embedded in and corrupted by random extraneous signals like thermal noise, electromagnetic interference, atmospheric noise, and electronic countermeasures. This means that the desired signal must be greater than the interfering signals after processing by the receiver for proper information about the target to be extracted.

The primary function of radar is to detect the presence of a target and noise energy limits the detection of weak signals. The weakest signal the receiver is able to detect is defined as the minimum detectable signal. Threshold detection requires establishing a threshold level that is below where useful signals are expected and the signal threshold level must be set at an appropriate level so the signal envelope does not exceed the threshold if noise exceeds the signal.[7]

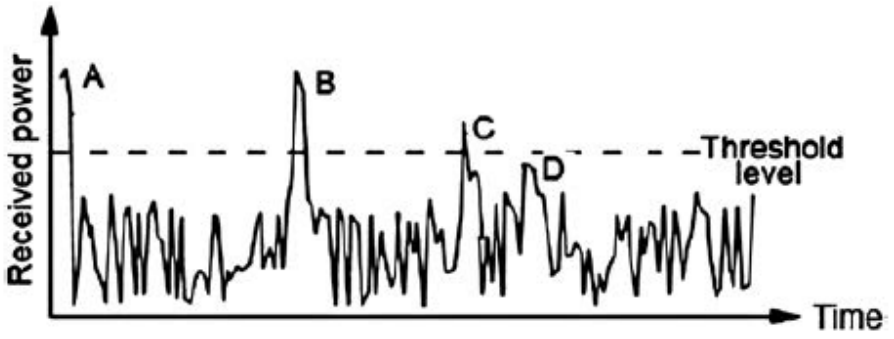

Figure 2. Typical envelope of radar receiver[4]

The delay of the returned echo provides information on the range. Commonly, a train of rectangular pulses with narrow width is used for range measurement as the pulse represents transmission and the shorter triangular pulse received is the echo signal from the target. The range R is calculated by first measuring the time delay and then multiplying it by the speed of light c before dividing that value by 2 to get the one-way range:

$$R = ct_d/2 \qquad (7)$$

A pulsed radar transmits and receives pulse trains with time period or pulse repetition interval T and pulse width τ. The inverse of the pulse repetition interval T is the pulse repetition frequency

$$f_r = 1/T \qquad (8)$$

and the duty cycle d_t is expressed by

$$d_t = \tau/T \qquad (9)$$

so the average transmitted power is then

$$P_{av} = P_t d_t = P_t \tau/T = P_t \tau\ f_r \qquad (10)$$

where P_T is the peak power transmitted by the radar. This makes the pulse energy

$$E_p = P_t \tau = P_{av} T = P_{av}/f_r. \qquad (11)$$

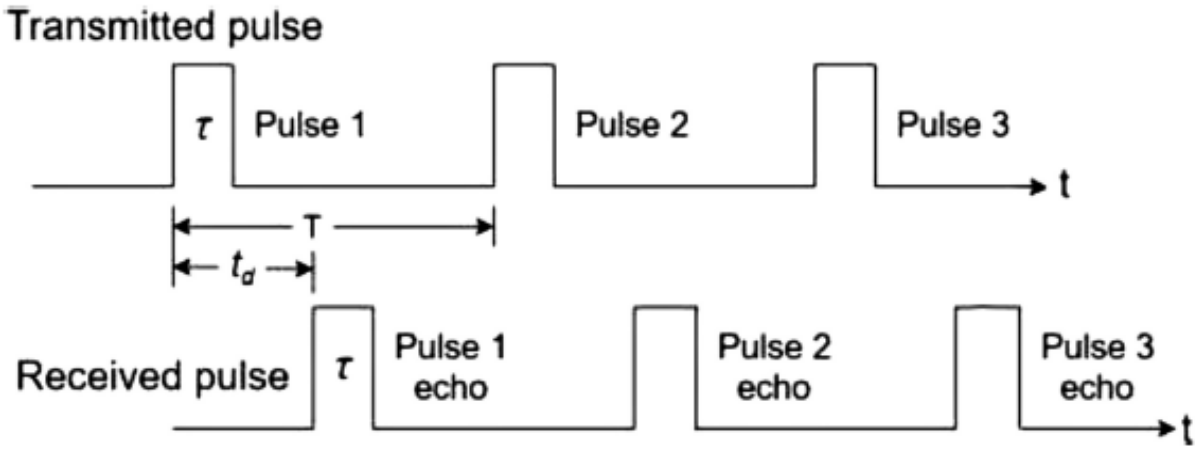

Figure 3. Transmitted and received pulse[4]

There must be sufficient time for any echo signals to return and be detected by the radar after a pulse is transmitted. Thus, the rate that pulses can be transmitted is limited to the longest range that targets are expected. When the repetition rate is too high, echo signals may return after the second pulse was transmitted, creating ambiguity in range measurement through second-time-around echoes. The range beyond which targets appear is called the maximum ubiquitous range, given by

$$R_u = \frac{c}{2f_r}. \qquad (12)$$

The ability to identify separate targets at the same angular position is called range resolution. The four dimensions used for target resolution are range, horizontal cross-range, vertical cross-range, and Doppler shift. A wider signal bandwidth improves the resolution of the radar and the range resolution is given by

$$\Delta R = \frac{c\tau}{2} = \frac{c}{2B} \qquad (13)$$

where B is the transmitted matched filter bandwidth in hertz.

If the source of oscillation or the observer of oscillation is in motion, there will be an apparent shift in frequency called the Doppler effect. The frequency shift or Doppler frequency provides information on the radial velocity. A reflected signal from a target in motion will cause a Doppler shift in the received echo. The Doppler shift provides information about the radial velocity of targets as well as various targets that may be occurring at the same time at different velocities.[7] The Doppler shift is positive when targets are approaching the radar and negative when targets are moving away from the radar. The Doppler shift is calculated as

$$f_d = f_0^{'} - f_0 \text{ Hz} \qquad (14)$$

where $f_0^{'}$ is the frequency of the returned echo and f_0 is the frequency of the transmitted signal from the radar.

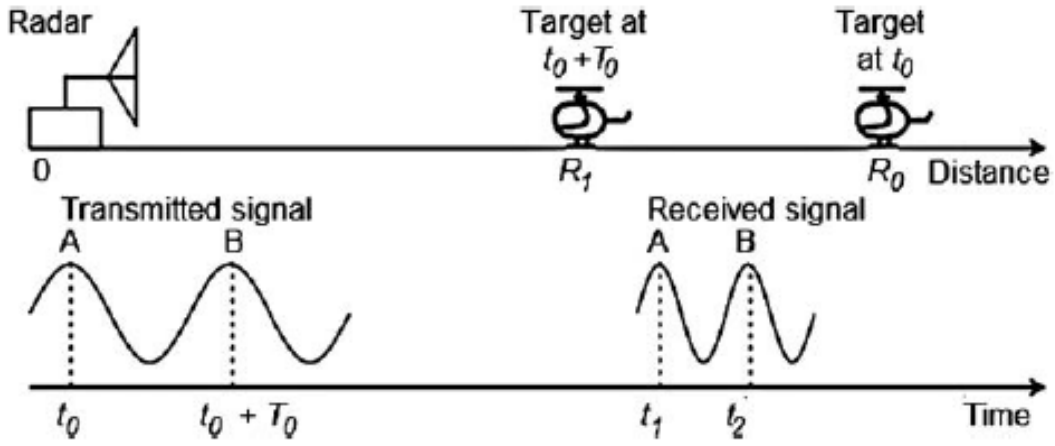

Figure 4. Transmitted and received waveforms of Doppler shift[4]

Assume a radar is transmitting with frequency f_0 and time period T_0, and a target is moving at constant radial velocity v_r toward the radar. For this discussion, the velocity v is equal to v_r, the first crest of the wave is transmitted at $t = t_0$, and the target is located at range $R = R_0$. The second crest of the wave is transmitted at time $t = t_0 + T_0$ to a target located at range $R = R_1$, where T_0 is the period of the transmitted wave. The duration of time ΔT required for the first crest on the wave to arrive at the target is

$$\Delta t = \frac{R_0 - v\Delta t}{c} \simeq \frac{R_0}{c+v}. \qquad (15)$$

Since the total round trip time for the first crest to return to the radar is $\frac{2}{\Delta T}$, it returns at time

$$t_1 = t_0 + \frac{2R_0}{c+v} \qquad (16)$$

And the second crest returns at time

$$t_2 = t_0 + T_0 + \frac{2R_1}{c+v}. \qquad (17)$$

Therefore, the period of the received signal is the difference $t_2 - t_1$ which is written as

$$T_0^{'} = T_0 - \frac{2(R_0 - R_1)}{c+v} = T_0(\frac{c-v}{c+v}) = T_0(\frac{1-v/c}{1+v/c}) \qquad (18)$$

Because $vT_0 = R_0 - R_1$, the quantity $(\frac{c-v}{c+v})$ represents the the dilation factor, the received frequency of the echo signal is the reciprocal of the corresponding time period given by

$$f_0^{'} = f_0(\frac{1+v/c}{1-v/c}). \qquad (19)$$

since $v/c << 1$, $f_0^{'}$ can be expanded binomially and simplified as shown below

$$f_0^{'} = f_0(1 + \frac{v}{c})(1 + \frac{v}{c} + \frac{v^2}{c^2} + \ldots) \simeq f_0(1 + \frac{v}{c})^2 \simeq f_0(1 + \frac{2v}{c}) = f_0 + \frac{2v}{\lambda} \quad (20)$$

where $\lambda = \frac{c}{f_0}$.

The Doppler shift now represents the shift of the received wave by the transmitted wave as

$$f_d = \frac{2v}{\lambda} = \frac{2v_r}{\lambda} = \frac{2v_r f_0}{c}. \qquad (21)$$

When the actual velocity is not equal to the radial velocity, the Doppler shift is modified to

$$f_d = \frac{2v}{\lambda} cos\gamma = \frac{2v}{\lambda} cos\gamma_\theta cos\gamma_\phi \qquad (22)$$

where γ_θ and γ_ϕ are the vertical and horizontal angles between the radar axis and target velocity and γ is the total angle the target direction makes with the radar line of sight.

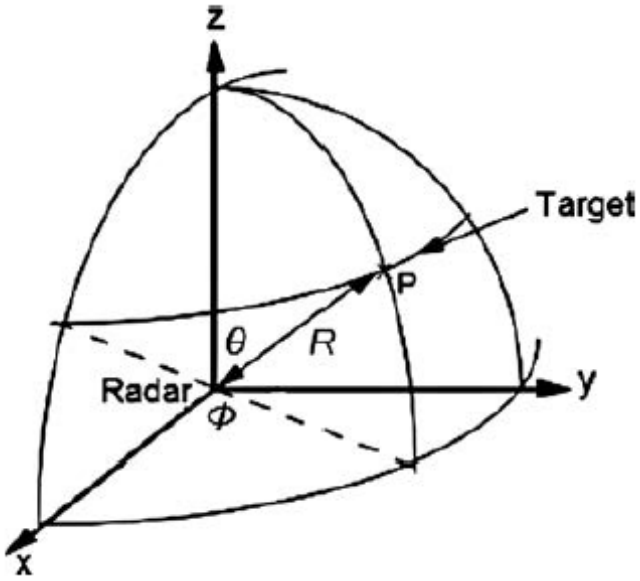

Figure 5. Target position in spherical coordinates[4]

In spherical coordinates (R, Θ, Φ), the radar is located at (0,0,0) and the target is located at (R, Θ, Φ). R is the range of the target, Θ is the angle the R vector makes with the origin in reference to the z-axis, and Φ is the angle the projection of the R vector makes with the x-y plane in reference to the x-axis. The pointing direction of the antenna informs the azimuth and elevation of the target relative to the radar. The elevation angle is represented by

$$\gamma = 90 - \Theta \qquad (23)$$

and is the angle between the antenna beam position and the local vertical through the center of the antenna. The azimuth angle is the angle the antenna beam makes on the local horizontal plane that passes through the antenna's center and perpendicular to the earth's surface.

MATHEMATICAL DESCRIPTION

The radar equation is a mathematical relationship that accounts for the effects of each major parameter of a radar system, target, target background propagation path, and medium. While it is useful for determining the maximum target distance of the radar, it is also a great tool for radar analysis, design, and operation. Real-life radar use demonstrates that there is imperfect knowledge of radar and target parameters and many loss factors must be accounted for to align performance and results.[8]

If a transmitter generates P_t watts of power that gets delivered to an isotropic antenna that radiates the EM energy uniformly in all directions, the constant power density $\widehat{p}_t'$ at distance R in a lossless propagation medium is equal to the transmitter power divided by the surface area of an imaginary sphere of radius R:

$$\widehat{P}_t' = \frac{P_t}{4\pi R^2}. \quad (24)$$

Radar uses directional antennas instead to concentrate the power density in a desired direction. The gain of an antenna measures the increased power radiated in the desired direction compared to the power that would have radiated from an isotropic antenna. Gain can be described as the ratio of intensity in the direction of maximum radiation to the radiation intensity from a lossless, isotropic antenna. The gain of a directional antenna is expressed by

$$G_t = \frac{4\pi A_t}{\lambda^2} \quad (25)$$

where A_t is the antenna effective aperture and λ is the wavelength of the transmitted signal. The relationship between the effective aperture area A_t and its actual area is

$$A_t = \rho_a A, \qquad 0 \leq \rho_a \leq 1 \quad (26)$$

where ρ_a is the antenna efficiency. If $\rho_a = 1$, the power density at the target, distance R from the radar with a directional antenna with transmitting gain G_t is

$$\hat{p}_t = \frac{P_t G_t}{4\pi R^2}. \quad (27)$$

The amount of energy scattered by the target is dependent on many parameters such as target size, orientation, shape, and material. All of these parameters are factored into the radar cross section, RCS (σ). RCS represents the ability of the target to scatter incident energy and is defined as 4π times the ratio of the power per unit solid angle reflected by the target in the direction of the radar to the power density of the incident wave at the target:

$$\sigma = 4\pi \frac{P_b/4\pi}{P_t/4\pi R^2} = 4\pi R^2 \frac{P_b}{P_t} \quad (28)$$

where $P_b/4\pi$ is the power per unit solid angle reflected in the direction of the radar. Therefore, the total reflected power by the target is

$$P_\sigma = \frac{P_t G_t \sigma}{4\pi R^2}. \quad (29)$$

If the reflected power is considered to be a uniform power source located at the target, the power density can be expressed as

$$\hat{p}_{\sigma} = \frac{P_t G_t \sigma}{4\pi R^2} \frac{1}{4\pi R^2} = \frac{P_t G_t \sigma}{(4\pi R^2)^2}. \quad (30)$$

Assuming that the area capturing the returned echo is equal to the effective area of the receiving antenna Ar, the total power received by the radar is given by

$$P_r = \frac{P_t G \sigma}{(4\pi R^2)^2} A_r. \quad (31)$$

And further assuming that the same antenna is used for transmission and reception as is for a monostatic radar and that $A_t = A_r = A_e$ and $G_t = G_r = G$ simplifies the total power received by the radar to

$$P_r = \frac{P_t G \sigma}{(4\pi R^2)^2} A_e = \frac{P_t G^2 \lambda^2 \sigma}{(4\pi)^3 R^4} \quad (32)$$

While this is a simple form of the wave equation, it is useful for rough approximations and requires the consideration of many factors such as radar systems losses for more realistic and accurate estimation. Thermal noise interferes with the ability of the receiver to detect the desired signal as it is randomly generated by electron motion in ohmic portions of the receiver input stages. The noise is directly proportional to the temperature of ohmic portions of the circuit at the antenna output terminal and the receiver bandwidth as given by

$$N_i = KT_e B \quad (33)$$

where $K = 1.38 \times 10^{-23}$ Joules/ degree Kelvin (Boltzmann's constant) and B is the receiver noise bandwidth at radar receiver input temperature T_e. The noise in a practical receiver is greater than the thermal noise so the noise at the output of the receiver can be considered to be equal to the thermal noise multiplied by a noise factor.[9] The noise factor F is defined as

$$F = \frac{N_0}{KT_0BG_a} = \frac{output\ noise\ of\ practical\ receiver}{output\ noise\ of\ ideal\ receiver\ at\ T_0\ (290K)} \quad (34)$$

where G_a is the power gain of the receiver or the ratio of output signal S_0 to the input signal S_i. The noise factor F can also be written as

$$F = \frac{S_i/N_i}{S_o/N_o} = \frac{(SNR)_i}{(SNR)_o} \quad (35)$$

where S, N, and SNR is denoted by i for input and o for output. By eliminating P_r in Eq. 32 using Eq. 35, the rearranged equation now yields

$$\frac{S_o}{N_o} = \frac{P_t G^2 \lambda^2 \sigma}{(4\pi)^3 R^4 FKT_0 B}. \quad (37)$$

However, losses such as within the system L_s, losses in propagation medium and path L_p, and losses due to multiple signal paths and ground reflections L_r, must be accounted for and can be incorporated into a term representing total signal loss $L = L_s L_p L_r$. Making this addition to the previous equation gives the output SNR or radar equation

$$\frac{S_o}{N_o} = \frac{P_t G^2 \lambda^2 \sigma}{(4\pi)^3 R^4 FKT_0 B} = \frac{P_t G^2 \lambda^2 \sigma}{(4\pi)^3 R^4 FKT_0 BL_S L_P L_R} = \frac{P_t G^2 \lambda^2 \sigma}{(4\pi)^3 R^4 FKT_0 BL}. \quad (38)$$

Alternatively, the equation can be rearranged to give the range given as

$$R = [\frac{P_t G^2 \lambda^2 \sigma}{(4\pi)^3 FKT_0 BL(S_o/N_o)}]^{1/4} \qquad (39)$$

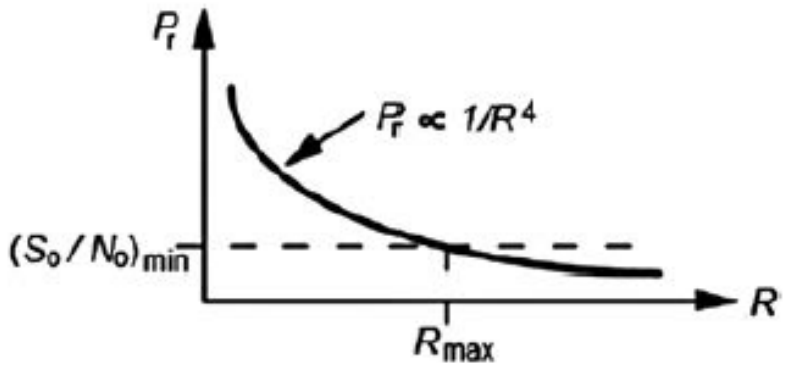

Figure 6. Received signal versus range[4]

The maximum detection range R_{max} corresponds to the minimum value of the output SNR, $(S_O/N_0)_{min}$, as shown in Figure 6. The output SNR is inversely proportional to the fourth power of range R and once a design is established for a given RCS, the range for unity output R_0 can be easily determined and

$$\frac{S_o}{N_o} = (\frac{R_o}{R})^4. \qquad (40)$$

REFERENCES

1. Watson-Watt, Robert. A History of Radar. Institution of Electrical Engineers, 1981.

2. "Radar in World War II." National WWII Museum, https://www.nationalww2museum.org/war/articles/radar-world-war-ii.

3. Kathren, Ronald L. and Warren H. Lewis. The Evolution of Radar. CRC Press, 2018.

4. Burrows, C. R. and S. S. Attwood. 1949. Radio Wave propagation. New York: Academic Press, Inc.

5. Rahman, Habibur. Fundamental Principles of Radar. Milton: CRC LLC, 2019. Web.

6. IEEE. 1974. “IEEE Standard Definitions of terms for Antennas.” IEEE Transaction on Antenna and Propagation 22, no. 1.1982.

7. Cummer, Steven A., and D. Keith Wilson. "Introduction to the Doppler Effect." Physics Today, vol. 66, no. 4, Apr. 2013, pp. 36-41. DOI: 10.1063/PT.3.1955.

8. Kingsley, Simon, and Shaun Quegan. Understanding Radar Systems. Berlin: Institution of Engineering and Technology, 1999. Web.

9. Nathanson, Fred E, J. Patrick Reilly, and Marvin Cohen. Radar Design Principles: Signal Processing and the Environment. 1999. Web.

MICRO-DOPPLER

Laser radar transmits light to an object and receives the reflected wave to measure various properties such as range and velocity. In coherent laser systems, phase information can be preserved but the slightest rotation or vibration can cause a Doppler frequency shift and significant phase change. In microwave radar systems, the micro Doppler-effect can be seen as those systems operate in a lower frequency range.

Oscillatory or micro motion can be described as any secondary motion of an object or its structural component such as rotating propellers, flapping bird wings, and human body parts. Human motion is very articulate and flexible so it is considered to be a complex micro motion of interest. Micro motion can induce Doppler frequency modulation around the carrier frequency of transmitted radar signals and the modulation frequency and intensity is determined by carrier frequency, rotation or vibration rate, and angle between vibration direction and the radar's line of sight.[1]

Knowing the frequency modulation allows for the determination of the kinematic properties of an object as a micro-Doppler signature is a distinctive characteristic. These signatures can be extracted using a continuous wave (CW) radar, but wide-band coherent Doppler radars are necessary to capture high resolution and to measure both range and Doppler information.

SIGNATURES

Rigid bodies have constant distances between distinguishable points in the object so that any rotation about a point can be described by rotation axis and angle. The Euler angles (ϕ, θ, ψ) represent rotations about three axes related to roll, pitch, and yaw. There are several points that must be specified in a rigid body in order for its motion to be completely defined:

- position
- linear velocity and acceleration
- angular velocity and acceleration
- linear and angular momentum

An example of a rigid body creating micro-Doppler signatures is the rotation of helicopter rotor blades as the rotating blades can be modeled as rigid, homogeneous, and linear rods rotating about a fixed axis at a constant rate.

A rotor with N blades rotating at constant angular velocity Ω through an angle $2\pi/N$ backscatters signals that will repeat from its original position so that the field is a periodic function of time with period $T_c = \frac{2\pi}{N_c \Omega}$.

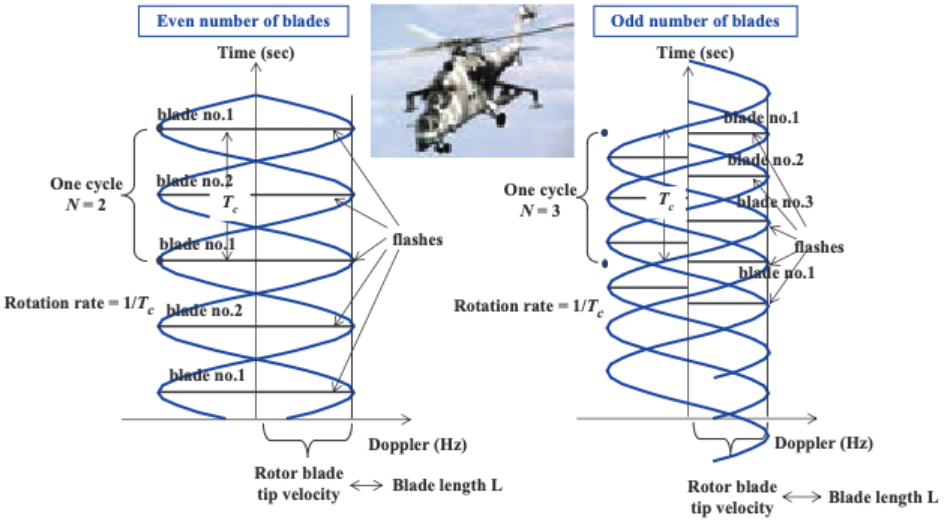

Figure 7. Micro-Doppler signature of helicopter rotor blades[1]

Depending on the number of blades present, the micro-doppler signature will be different. The signature allows for the estimation of number of blades, length of the blades, and rotation rate of the rotor.

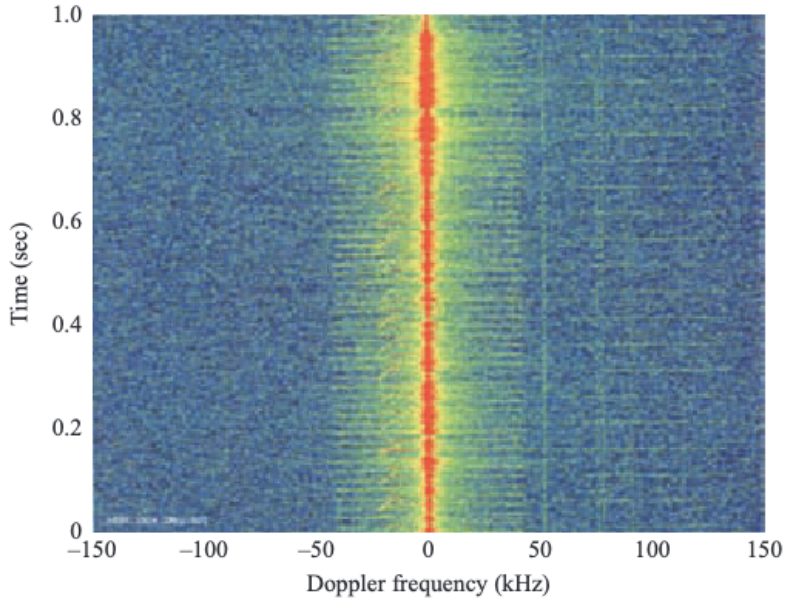

Figure 8. Micro-Doppler signature of helicopter tail and rotor blades[2]

The motion of a human body is generally considered to be nonrigid and articulated but the locomotive motion of limbs can be characterized as periodic. One of the most popular examples of this is the human gait cycle. The walking model uses time-dependent body trajectories. The trajectories, translational and rotational, describe the cycle of the walking motion and are dependent on the determined walking speed.

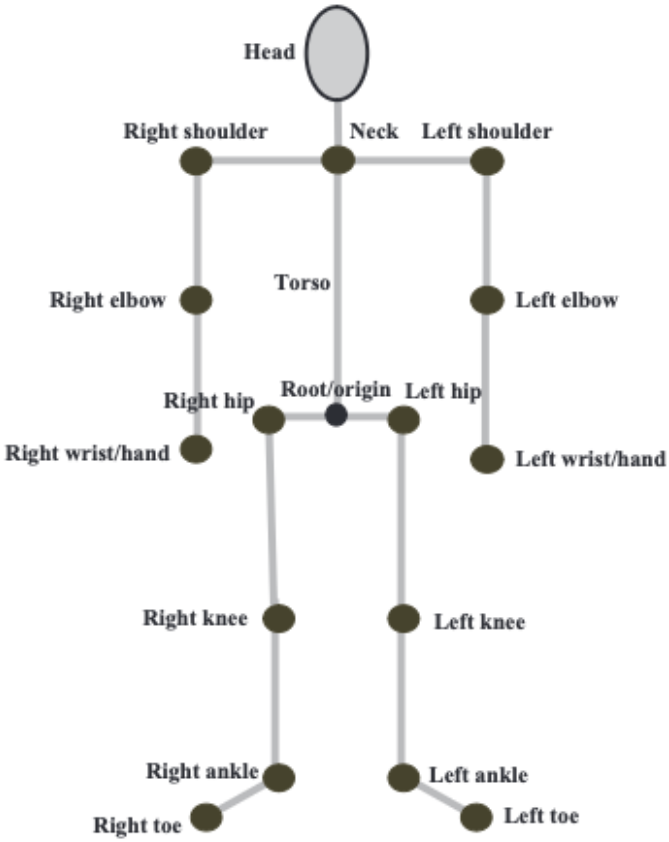

Figure 9. Seventeen joint human model[3]

The trajectories are used to calculate the location of 17 reference points on the human body depicted in Figure 9 and radar scattering from nonrigid body parts can be computed using the radar signatures of individual body parts since they can be modeled by isotropic point scatterers. The predetermined body model above models body parts

with simple geometric shapes like cylinders or ellipsoids so that the scattered RCS equation of each part can be used to calculate relative amplitude of returned signals.[3]

CHALLENGES AND PERSPECTIVES

There are several challenges in radar micro-doppler signature applications and research into successfully mapping signatures and body parts is difficult. The micro-Doppler signatures of a human gait must be decomposed into component signatures associated with the torso, arms, and feet.[4] Effective decomposition proves difficult as it requires the decomposition of these signatures into mono-components and the measurement of embedded kinematic/structural information. The Viterbi algorithm in the joint time-frequency domain has achieved some success, though.[6]

The detection of abnormal behavior is also a challenge researchers are tackling and it first requires the ability to learn what normal human movements are. The tracking of these movements and selection of relevant features becomes difficult as the complexity of human gait increases.[7]

A particular perspective of micro-doppler signature research that is relevant to sports is the combination of multiple bistatic radars to observe targets from different aspects. With multiple viewing angles, a combined micro-Doppler signature is obtained that is dependent on the topology of the radar system, location of the target, and direction of the target.[7] Combining information from multiple channels allows for finer measurement of various target properties and improved target recognition.[8]

Human-based activities might require the exploitation of the differences in micro-Doppler signatures to develop a better activity classifier as different movements produce different signatures. For example, the maximal Doppler shift of the torso signature, the offset from the principal Doppler shift, the maximum Doppler variation of the torso line, oscillation frequency of the motion, and the kinematic parameters of the limbs are all features of interest.

THEORY

If an object is in motion, the electromagnetic signal transmitted by radar reflects with a Doppler frequency shift that is determined by the radial velocity of the object and the wavelength used by the radar. The roundtrip Doppler shift is given by $f_D = - f * 2v/c$ where c is speed of wave propagation, f is radar transmitted carrier frequency, and v is velocity of the object along the line of sight of the radar. v is positive when the object is moving away from the radar and negative when the object is moving toward the radar. This means that the Doppler frequency change is negative when the object is moving away from the radar. Additionally, v is determined as the relative velocity in situations when the radar is also moving.

Any rotation, vibration, or translational motion of the object will result in micro motions that will induce frequency modulation on the reflected signal with side-bands about the Doppler shifted carrier frequency due to translation. This defines the micro-Doppler effect and it was first observed in coherent laser systems and microwave radars. High

resolution and time-frequency analysis can be used to exploit micro-Doppler signatures to classify an object and its movement.

The micro-Doppler effect can be formulated in mathematics and derived by applying micro motions to the conventional Doppler effect.[9] For free-form deformation, each particle moves from an initial position P to a new position $P_t = f(t, P)$. Simple models compute the deformation with jointly connected rigid body parts. Non-rigid bodies are modeled as several connected rigid body segments and the motion of each segment is treated as a rigid body motion.[10]

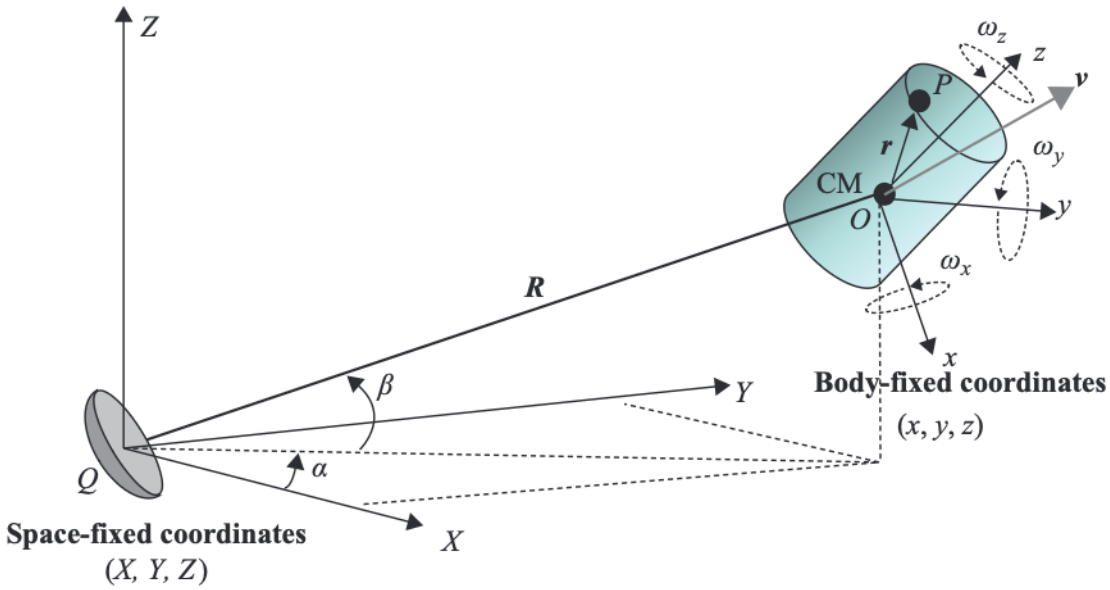

Figure 10. Space and body fixed coordinate system describing object motion[1]

A global (X, Y, Z) and a local (x, y, z) coordinate system is used to describe the motion of a rigid body (Figure 10). Range vector R is from the origin of the global or space-fixed system to the origin of the local or body-fixed system. With the origin of the local system

at the center of mass of the body and the orientation of the axes of the body-fixed system to the space-based system given by independent angles: α and β.

The rigid body becomes a mechanical system with six degrees of freedom and r denotes the position of arbitrary particle P in the body fixed system with its position in the space-based system is given by $R + r$ and its velocity given by

$$\frac{d}{dt}(R + r) = v + \Omega r \qquad (1)$$

where v is the translational velocity of the CM of the rigid body and $\Omega = (\omega_x, \omega_y, \omega_z)^T$ is the angular velocity vector of the body rotation where ω_x, ω_y, and ω_z are the angular rotation velocities about the body fixed x-, y-, and z-axis. Ω is in the direction along the axis of rotation and the rigid body motion consists of the translational motion and the micromotion.

Euler angles and rotation matrices are typically used to represent the orientation of an object as the rotation of a rigid body about an axis can be described by the axis and the rotating angle. Euler's rotation theorem says that any two independent orthonormal coordinates are related by a sequence of rotations about coordinate axes. The Euler angles or rotation angles ϕ, θ, and ψ are counterclockwise rotations about the z-, y-, and x- axis, respectively (Figure 11).[11]

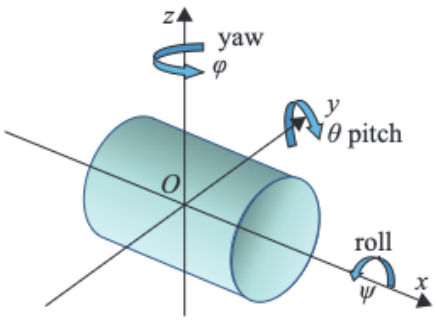

Figure 11. Roll-pitch-yaw convention[1]

Roll pitch and yaw are used to describe the rotation sequence x,y,z so that the x-axis is rolled by angle ψ, y axis pitched by angle θ, and z axis yawed by angle ϕ. This rotation matrix sequence is described by $R_{X-Y-Z} = R_X(\psi)R_X(\theta)R_X(\phi) =$

$$\begin{bmatrix} r_{11} & r_{12} & r_{13} \\ r_{21} & r_{22} & r_{23} \\ r_{31} & r_{32} & r_{33} \end{bmatrix}$$

where the components of the rotation matrix are

$$\begin{aligned} r_{11} &= -\sin\varphi\cos\theta\sin\psi + \cos\varphi\cos\psi \\ r_{21} &= -\cos\varphi\cos\theta\sin\psi - \sin\varphi\cos\psi \\ r_{31} &= \sin\theta\sin\psi \\ r_{12} &= \sin\varphi\cos\theta\cos\psi + \cos\varphi\sin\psi \\ r_{22} &= \cos\varphi\cos\theta\cos\psi - \sin\varphi\sin\psi \\ r_{32} &= -\sin\theta\cos\psi \\ r_{13} &= \sin\varphi\sin\theta \\ r_{23} &= \cos\varphi\sin\theta \\ r_{33} &= \cos\theta \end{aligned}$$

MICRO MOTION

The micro-Doppler effect can be derived by introducing micro motion to conventional Doppler analysis, typically by adding a new reference coordinate system (X', Y', Z') that shares the same origin as the object local coordinates.[9] This new coordinate system has the same translational motion as the object but has no rotation with respect to radar coordinates. An object with velocity v and angular rotation velocity vector $\overline{\Omega}$ can be represented by

$$\Omega = (\omega_x, \omega_y, \omega_z)^T = (\omega'_x, \omega'_y, \omega'_z)^{T'} \qquad (2)$$

If an object is represented as a set of point scatterers, a point scatterer P at time $t = 0$ and at point P' at time t can be described as a translation with velocity v and or a rotation from P'' to P' with angular velocity Ω. Movement observed in the reference coordinate system locates the point scatterer P at $r_0 = (X'_0, Y'_0, Z'_0)^T$ and rotation from P'' to P' is described by the rotation matrix R_t. Thus, the location of P' at time t is

$$R = O_t P' = R_t O_t P'' = R_t r_0 \qquad (3)$$

The range vector from the radar at Q to the scatterer at P' is derived by

$$QP' = QO = OO_t + O_t P' = R_0 + v_t + R_t r_0 \qquad (4)$$

And the scalar range becomes $r(t) = ||R_0 + v_t + R_t r_0||$

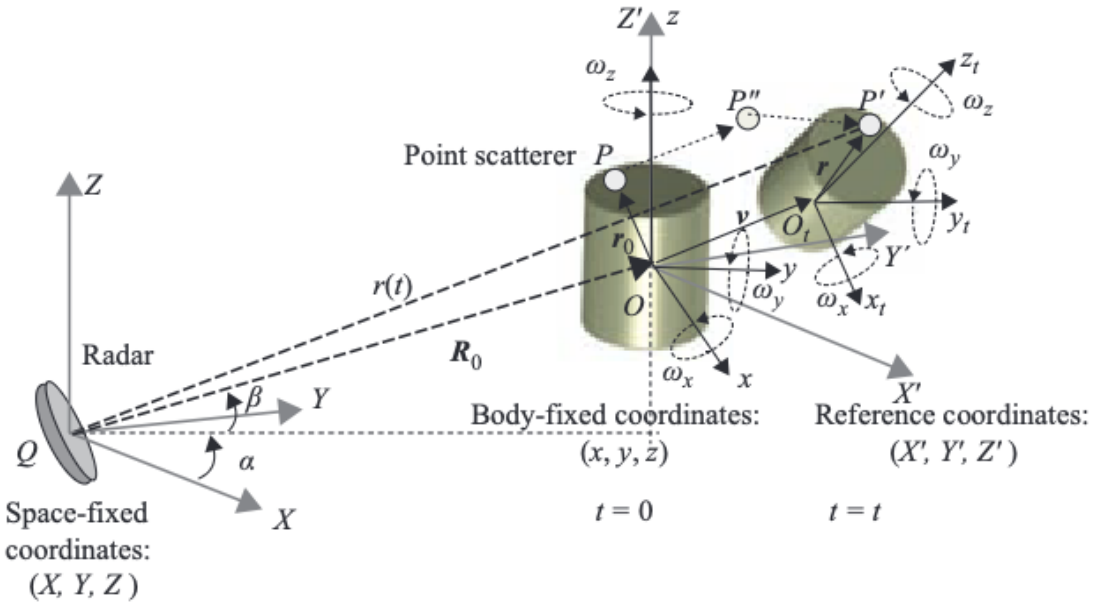

Figure 12. Geometry of radar and object with translation and rotation[1]

If the radar transmits a sinusoidal waveform with carrier frequency f, the signal returned from the point scatterer is a function of $r(t)$

$$s(t) = \rho(x,y,z)exp(j2\pi f\frac{2r(t)}{c}) = \rho(x,y,z)exp(j\overline{\Phi}(r(t)) \qquad (5)$$

where ρ is the reflectivity function of point scatterer P in object local coordinates and the base-band signal is

$$\Phi(r) = 2\pi f\frac{2r(t)}{c}. \quad (6)$$

The Doppler frequency shift induced by the object's motion it derived as:

$$f_D = \frac{1}{2\pi}\frac{d\overline{\Phi}(t)}{dt} = \frac{2f}{c}\frac{d}{dt}r(t)$$

$$= \frac{2f}{c}\frac{1}{2r(t)}\frac{d}{dt}[(\overline{R_0} + \overline{v}t + R_t\overline{r}_0)]$$

$$= \frac{2f}{c}[\overline{v} + \frac{d}{dt}(R_t\overline{r}_0)]^T \cdot \overline{n} \quad (7)$$

where $\bar{n} = \frac{\bar{R_0}+\bar{v}t+R_t\bar{r_0}}{||\bar{R_0}+\bar{v}t+R_t\bar{r_0}||}$ is the unit vector of $\overline{QP'}$.

To derive the Doppler shift induced by rotation, a useful relationship $\bar{u} \times \bar{r} = \widehat{ur}$ is used and the angular rotation velocity vector Ω rotates along the unit vector $\frac{\Omega}{\bar{\Omega}}$ with scalar angular velocity $|\bar{\Omega}| = \Omega$. Assuming the pulse repetition frequency to be high with relatively low angular velocity, the rotational motion during time t can be considered infinitesimal and the rotation matrix becomes

$$R_t = exp(\widehat{\omega t}) \qquad (8)$$

where $\widehat{\omega}$ is the skew symmetric matrix associated with $\bar{\Omega}$. The Doppler frequency shift then becomes

$$f_D = \frac{2f}{c}[\bar{v} + \frac{d}{dt}(exp(\widehat{\omega t})\,\bar{r}_0]^T \cdot \bar{n}$$

$$= \frac{2f}{c}(\bar{v} + \widehat{\omega} exp(\widehat{\omega t})\,\bar{r}_0)^T \cdot \bar{n}$$

$$= \frac{2f}{c}(\bar{v} + \bar{\Omega} \times \bar{r})^T \cdot \bar{n}. \qquad (9)$$

If $|R_0| >> |\bar{v}t + R_t\bar{r}|$, $\bar{n}$ can be approximated as $\bar{n} = \frac{\bar{R_0}}{|\bar{R_0}|}$, which is the direction of the radar line of sight, and the Doppler frequency shift is approximately

$$f_D = \frac{2f}{c}(\bar{v} + \bar{\Omega} \times \bar{r}) \cdot \bar{n} \qquad (10)$$

Where the first term $\frac{2f}{c}\bar{v} \cdot \bar{n} = f_{trans}$ is the Doppler shift due to the object's translation and the second term $\frac{2f}{c}(\bar{\Omega} \times \bar{r}) \cdot \bar{n} = f_{mD}$ is the micro-Doppler shift due to rotation. If

the rotation is time varying, the angular rotation velocity is a function of time that can be expressed by

$$\overline{\Omega}(t) = \overline{\Omega_0} + \overline{\Omega_1} t + \overline{\Omega_2} t^2 + \ldots \qquad (11)$$

and if no more than second order terms are considered, the micro-Doppler shift can be expressed by

$$f_{mD} = \frac{2f}{c} [\overline{\Omega}(t) \times \bar{r}] \cdot \bar{n} = \frac{2f}{c} [\overline{\Omega_0} \cdot (\bar{r} \times \bar{n}) + \overline{\Omega_1} \cdot (\bar{r} \times \bar{n}) t + \overline{\Omega_2} \cdot (\bar{r} \times \bar{n}) t^2. \qquad (12)$$

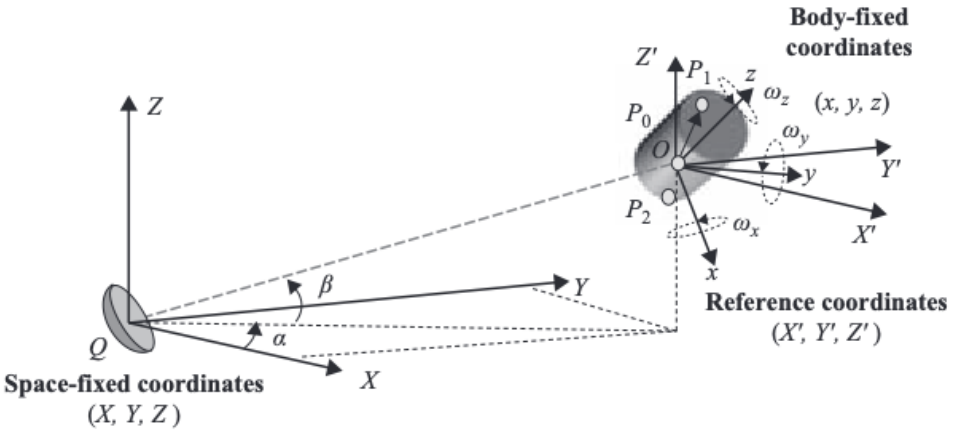

Figure 13. Geometry of radar and rotating object[1]

Any point on a rotating object will move to a new position (X', Y', Z') that is calculated by multiplying the initial position vector with a rotation matrix.The rotation matrix can be the commonly used z-y-x rotating sequence that rotates ϕ_0 about the z-axis, θ_0 about the y-axis, and ψ_0 about the z-axis again. This rotation matrix is defined by

$$R_{init} = R_z \phi_0 \cdot R_x \theta_0 \cdot R_z \psi_0 \qquad (13)$$

In the local object coordinate system, a point scatterer P at $r_P = [x_P, y_P, z_P]^T$ rotates with angular velocity $\omega_P = [\omega_x, \omega_y, \omega_z]^T$ and will move to a new location in the reference coordinates by $R_{init} \cdot r_P$. The unit vector of the rotation is

$$\overline{R_{init}} \cdot \frac{\Omega}{|\Omega|} = \omega' = (\omega_x', \omega_y', \omega_z')^T \quad (14)$$

and applying the Rodrigues formula at time t makes the rotation matrix

$$R_t = I + \widehat{\omega}' sin\Omega t + \widehat{\omega}'^2(1 - cos\Omega t) \quad (15)$$

where $\widehat{\omega}'$ is a skew symmetric matrix.

In the reference coordinate system (X', Y', Z') at time t, point scatterer P will move to a new location $r = R_t \cdot R_{Init} \cdot r_P$ and the micro-Doppler frequency shift induced by rotation is approximated as

$$f_{mD} = \frac{2f}{c}[\Omega\overline{\omega}' \times \overline{r}]_{radial} = \frac{2f}{c}(\overline{\Omega\widehat{\omega}'}\overline{r})^T \cdot \overline{n} = \frac{2f}{c}[\overline{\Omega\widehat{\omega}'}R_t \cdot \overline{R_{Init}} \cdot \overline{r_P}]^T \cdot \overline{n} \quad (16)$$

If the skew symmetric matrix associated with ω' is defined by a unit vector, then $\widehat{\omega}'^3 = \widehat{\omega}'$ and the rotation induced micro-Doppler frequency becomes

$$f_{mD} = \frac{2f\Omega}{c}[\widehat{\omega}'(\widehat{\omega}' sin\Omega t + I cos\Omega t)\ \overline{R_{Init}} \cdot \overline{r_P}]_{radial}. \quad (17)$$

REFERENCES

1. Chen, Victor C, David Tahmoush, and William J Miceli. Radar Micro-Doppler Signatures: Processing and Applications. Vol. 34. Stevenage: Institution of Engineering and Technology, 2014. IET Radar, Sonar and Navigation Ser. Web.

2. Yang, S.Y., Yeh, S.M., Bor, S.S., Huang, S.R., and Hwang, C.C., ‘‘Electromagnetic backscattering from aircraft propeller blades,’’ IEEE Transaction on Magnetics, vol. 33, no. 2, pp. 1432–1435, 1977.

3. Boulic, R., Thalmann, M.N., and Thalmann, D., ‘‘A global human walking model with real-time kinematic personification,’’ The Visual Computer, vol. 6, no. 6, pp. 344–358, 1990.

4. van Dorp, P. and Groen, F.C.A., ‘‘Human walking estimation with radar,’’ IEE Proceedings Radar, Sonar and Navigation, vol. 150, pp. 356–365, 2003.

5. Thayaparan, T., Stankovic, L., and Djurovic, I., ‘‘Micro-Doppler-based target detection and feature extraction in indoor and outdoor environments,’’ Journal of the Franklin Institute, vol. 345, no. 6, pp. 700–722, Sep. 2008.

6. Li, P., Wang, D.C., and Wang, L., ‘‘Separation of micro-Doppler signals based on time frequency filter and Viterbi algorithm,’’ in Signal, Image and Video Processing, Springer, Sep. 2011.

7. Smith, G.E., Radar Target Micro-Doppler Signature Classification, PhD Dissertation, Department of Electronic and Electrical Engineering, University College London, 2008.

8. Smith, G.E., Woodbridge, K., Baker, C.J., and Griffiths, H., ‘‘Multistatic micro-Doppler radar signatures of personnel targets,’’ IET Signal Processing, vol. 4, no. 3, pp. 224–233, 2010.

9. Chen, V.C., The Micro-Doppler Effect in Radar, Artech House, Boston/London, 2011.

10. Shabana, A.A., Dynamics of multibody systems, (3rd ed.), Cambridge University Press, Cambridge, UK, 2005.

11. Goldstein, H., Poole, C., and Safko, J., Classical Mechanics, (3rd ed.), Addison-Wesley, Boston, NY, 2002.

12. Huang, N.E., et al., ‘‘The empirical mode decomposition and the Hilbert spectrum for nonlinear and non-stationary time series analysis,’’ Proceedings Royal Society London, series A, vol. 454, 1998, pp. 903–995.

13. Gabor, D., ‘‘Theory of communication,’’ Journal IEE (London), vol. 93, Part III, no. 26, 1946, pp. 429–457.

TRACKMAN

OVERVIEW

Trackman technology utilizes cutting-edge Doppler radar and club and ball tracking technology to accurately measure and report data such as club delivery, ball launch, ball flight, and tracing. As of January 1st 2021, over 1,000,000,000 shots have been hit in front of a Trackman and sent up to the data cloud. Additionally, over half of the 1,000,000,000 shots were taken in the year prior.[1] Users have gained access to statistical data that uncovers how and why the ball moves as TrackMan technology has the ability to capture data such as club speed, ball speed, launch angle, spin rate, spin axis, apex, carry and more. The advanced aerodynamic models can also determine the impact of environmental factors such as wind, weather, and altitude.[2]

One of Trackman's mantras, "Data needs to be actionable," properly represents their determination for the minimum accuracy of various parameters in order to make objective recommendations on a player's performance. Their current product line comfortably meets all of the recommended parameter accuracy.[1]

The newest Trackman model, Trackman 4, relies on Optically Enhanced Radar Tracking technology (OERT) that synchronizes two radar systems and a built-in camera. One of the radar systems is focused on capturing club and impact data, which has made significant increases in the data that can be gathered about putting strokes. The other radar is set up for long-range tracking of the ball path. This provides the best of both

worlds as radar provides full 3D flight ball tracking, robust tracking in all weather conditions, superior velocity, spin rate, and range accuracy from transmitting at various frequencies at an extremely high sampling rate. Optical capabilities enable pixel tracking that is accurate enough to produce ball and club tracking and intuitive verification of data accuracy with video evidence.[4]

A brand new Trackman 4 unit starts at $20,000 and a used version of previous models can sell for up to $15,000 still. While some recreational golfers might decide to splurge on a personal Trackman, the units are more often found at driving ranges, golf learning centers, and professional tournaments. Club manufacturers use Trackman data to better design clubs that perform better under certain conditions or certain player types.

PGA TOUR

In 2022, the PGA Tour selected Trackman tracking and tracing to enhance how fans experience the world's best golfers with metrics and data provided digitally. This agreement doubles past ball-in-motion tracing capabilities as it allows almost every shot to be traced and shared to television and OTT partners across various platforms. Their goal is to create an exciting future of golf that can be told in innovative ways to take the fan experience to the next level. The new technology expands current capabilities to include shots hit from the fairway as well as tee shots and locking onto a ball that is obstructed until mid-flight. A typical TOUR event consists of about 40 Trackman units placed around the course at tee boxes and greens to capture final resting position. By doubling the collection of radar information, the new system substantially increases the range of content that can be layered with video across PGA TOUR media platforms.[5]

Klaus Eldrup-Jorgensen, co-founder and CEO of TrackMan, commented “We have been working closely with the PGA TOUR for more than 15 years, to accurately measure and report data on club delivery, ball launch, ball flight, and tracers for the best players in the world. We are proud to be chosen to implement our new solutions with the PGA TOUR, which will ultimately include all shots for all players. The future of golf will be told in new and innovative ways, the fan experience will elevate to a new level, and the stories about how good these guys play is just beginning.”[5]

Trackman has become a valuable element to Shotlink powered by CDW, which is the PGA TOUR’s real-time data collection and scoring system. This scoring system has transformed how tournaments, broadcast partners, players, and fans are able showcase a larger part of the sport and Trackman system enables Shotlink to auto-trigger on shots without any human input. Its capabilities also enable the ability to lock on a ball that starts behind trees before becoming visible mid-flight and accurate tracking of balls up to 400 yards in various weather conditions such as rain, fog, sunrise, and sunset.

SCIENCE

The collision moment of a golf ball is only about half a millisecond long and Trackman is capable of reporting data at maximum compression at the geometric center of the golf club in order to ensure ultra-high precision tracking. Trackman’s accuracy tolerance for spin measurement of the golf ball is 20 rpm, which is less than 1% the spin rate of a typical driver shot.[1]

Trackman's mantra is, "When possible, always measure the actual ball flight," but sometimes it is not possible since many golfers use the trackman indoors. In indoor settings, Trackman's sophisticated aerodynamic ball flight model that has been calibrated with millions of shots is used to project the entire flight and roll of the ball. The accuracy of ball launch conditions is critical for Trackman because any error will be magnified down range.

		NORMALIZED							
	Actual	25C,0m	diffAct	35C,0m	diffAct	*diff25C/0m*	25C,500m	diffAct	*diff25C/0m*
Driver	**265.7**	261	-4.7	265.7	0	*4.7*	267.9	2.2	*6.9*
3wood	**248.5**	239.8	-8.7	244	-4.5	*4.2*	246	-2.5	*6.2*
3wood,tee	**254.6**	242.6	-12	247.7	-6.9	*5.1*	250.2	-4.4	*7.6*
4i	**205.8**	197.3	-8.5	201.2	-4.6	*3.9*	203	-2.8	*5.7*
5i	**196.7**	186.5	-10.2	190.7	-6	*4.2*	192.7	-4	*6.2*
6i	**181.7**	170.7	-11	174.9	-6.8	*4.2*	176.9	-4.8	*6.2*
7i	**173.2**	159.2	-14	163.1	-10.1	*3.9*	165.1	-8.1	*5.9*
8i	**157.1**	146.4	-10.7	149.9	-7.2	*3.5*	151.8	-5.3	*5.4*
9i	**146**	133.8	-12.2	137.1	-8.9	*3.3*	138.7	-7.3	*4.9*
PW	**131.2**	120.8	-10.4	123.5	-7.7	*2.7*	124.9	-6.3	*4.1*

Figure 14. Trackman normalization across ranging environmental conditions[1]

The normalization feature Trackman offers is able to adapt the measured data from outdoor shots to the same indoor ball flight model to gather true swing and ball data that is unaffected by environmental conditions such as wind, temperature, and altitude. The above test data shows the distance the golf ball was hit in several conditions: actual conditions, 25 degrees Celsius at sea level, 35 degrees Celsius at sea level, and 25 degrees Celsius at 500 m elevation. This normalization feature can be particularly useful for golfers preparing to play in an unfamiliar environment and testing golf club settings to maximize on-course performance.

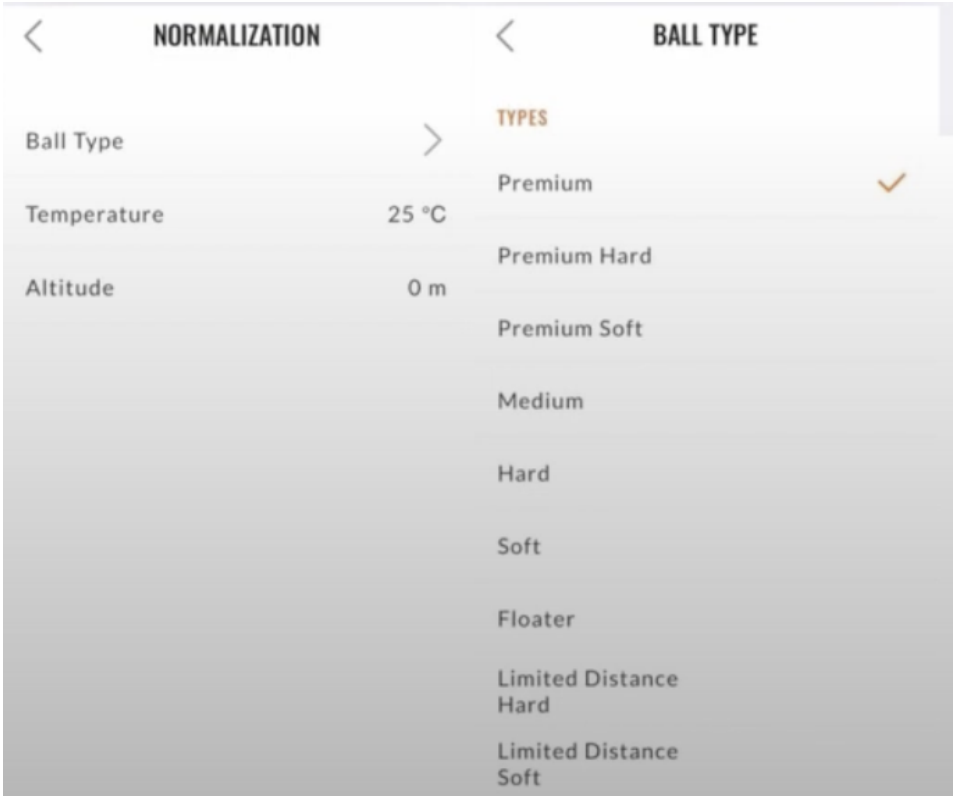

Figure 15. Normalization options including environment and ball type[1]

Another element of the normalization feature is the ability to convert the poorer performance of a range ball to the ideal performance of the ball of preference, which will provide more insights that can be translated to competitive play. This feature is extremely useful for club fitting sessions that occur under unfavorable weather conditions such as 20 mph headwinds. This allows the golfer to get fit for the proper clubs as the data will be adapted for normal playing conditions.

IMPACT POSITION

This radar spectrogram showcases the velocity of a golf ball over the entire duration of the ball travel. It is seen that the frequency emitted to the ball shifts as the measured

velocity is dependent on the flight of the ball. The left side of the graph features the impact of the golf ball and the right side of the graph features the ball landing and rolling out before coming to a stop.

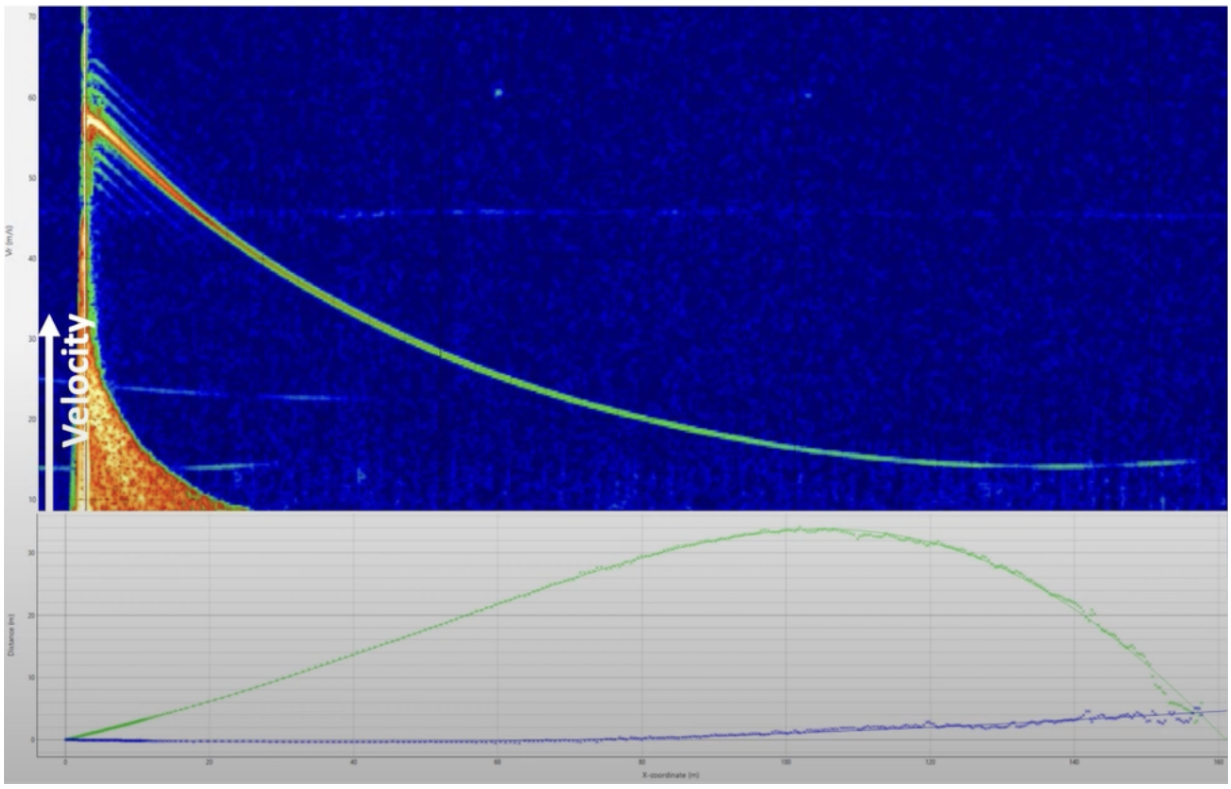

Figure 16. Trackman spectrogram of hit golf ball[1]

Figure 17 showcases about 60 milliseconds of club-ball impact, as the left side of the spectrogram showcases the delivery of the club to the ball and the right side portrays the deceleration of the clubhead after impact as well as the acceleration the impacted ball. Since the Trackman is located behind the golfer, its spectrogram is able to capture the relative velocity difference between the club and toe. Trackman considers their radar as 4-dimensional since it tracks velocity, vertical angle, horizontal angle, and distance. The synchronized 2-dimensional camera takes captures indicated by the yellow lines for club and shaft tracking to combine with radar data for impact location determination.

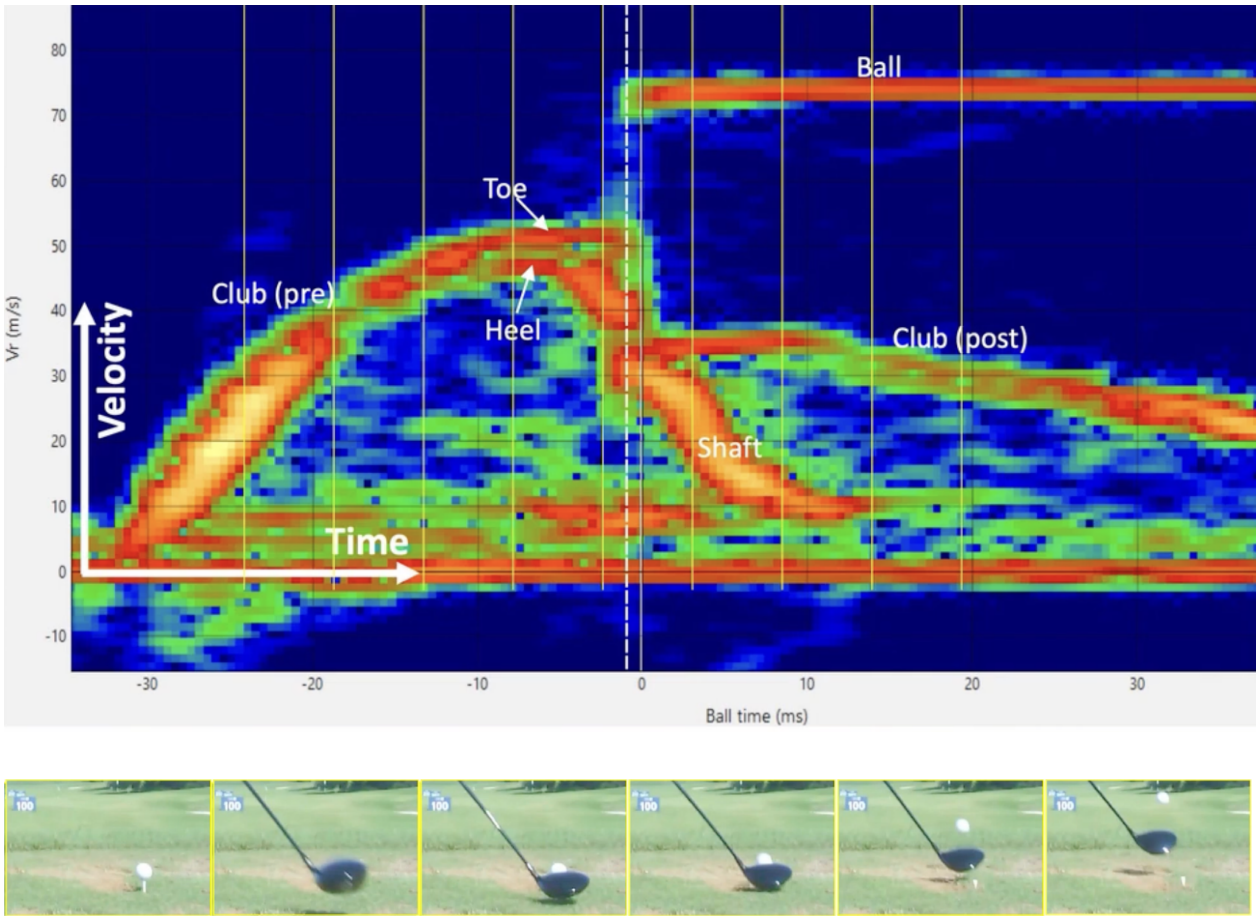

Figure 17. Trackman spectrogram at impact and synced swing path images[1]

Four parameters are required for the impact location to be determined: ball position before impact, precise time of impact, position of the club head, and the center position of the club face markers (groove lines).[6] The ball position is characterized by a combination of radar and camera and the time of impact is determined by the Trackman's ultra high sampling rate of 40,000 samples per second. The OERT process creates a 4-dimensional silhouette of the clubhead and the virtual clubface is defined by an offset in relation to the hosel of the club. Since this offset does not differ significantly between club models, the standard values will be sufficient but the software allows for changes if necessary.

Figure 18. Trackman visualization of impact position[1]

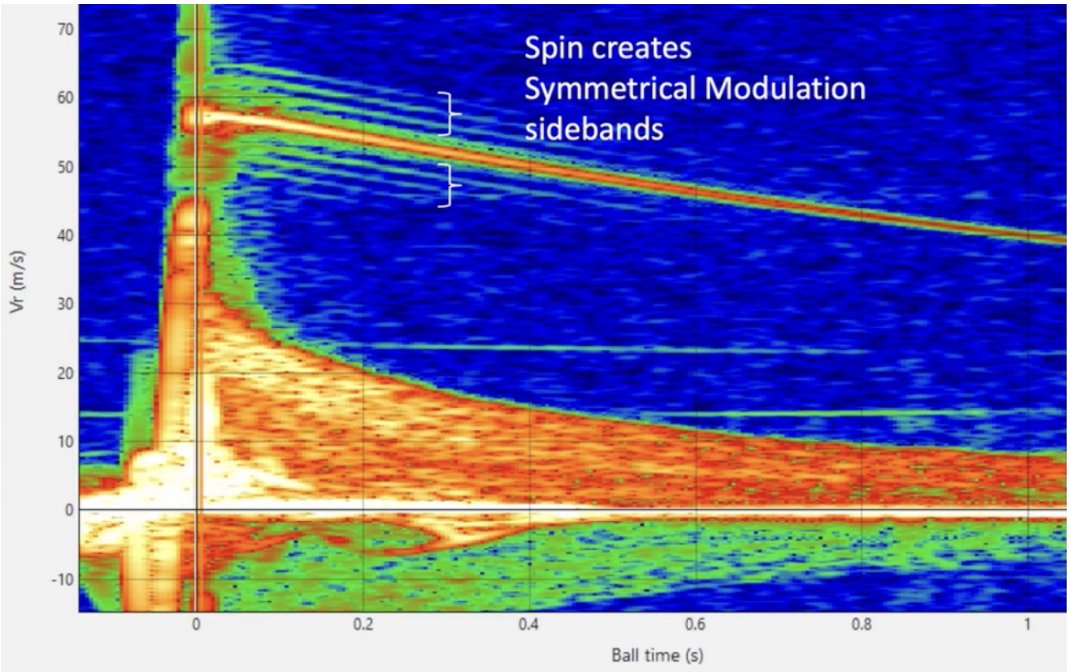

Figure 19. Trackman spectrogram at impact with distinct spin sidebands[1]

Figure 19 depicts the club-ball impact and the initial launch of the ball with the clearly defined orange streak across the top of the graph. Along the ball signature are parallel symmetric lines of the sides of the ball that are spaced at exactly the spin frequency of the ball. They are not always this clear so it takes special processing to get a high pickup rate for proper measurement. Because the ball flight of balls hit indoors is so short, a metallic dot on the ball allows for amplification of the signal for more accurate spin rate data.

TRAINING FEATURES

Performance Putting is one of Trackman's newest features that allows users to now track the entire length of a putt, eclipsing previous technology that was only able to collect data after the first foot or two. Performance Putting provides versatile training options to users to analyze areas of greatest improvement to them. Trackman has developed three evaluations as part of their Performance Putting software that enables students and coaches to analyze areas of improvement: launch direction, speed control, and total putt evaluation.[7]

The launch direction of a putt is vital as it must start on line to the whole. A common practice technique involves gates, but Trackman uses geometry to identify allowable tolerances dependent on the length of the putt, hole size, and speed.

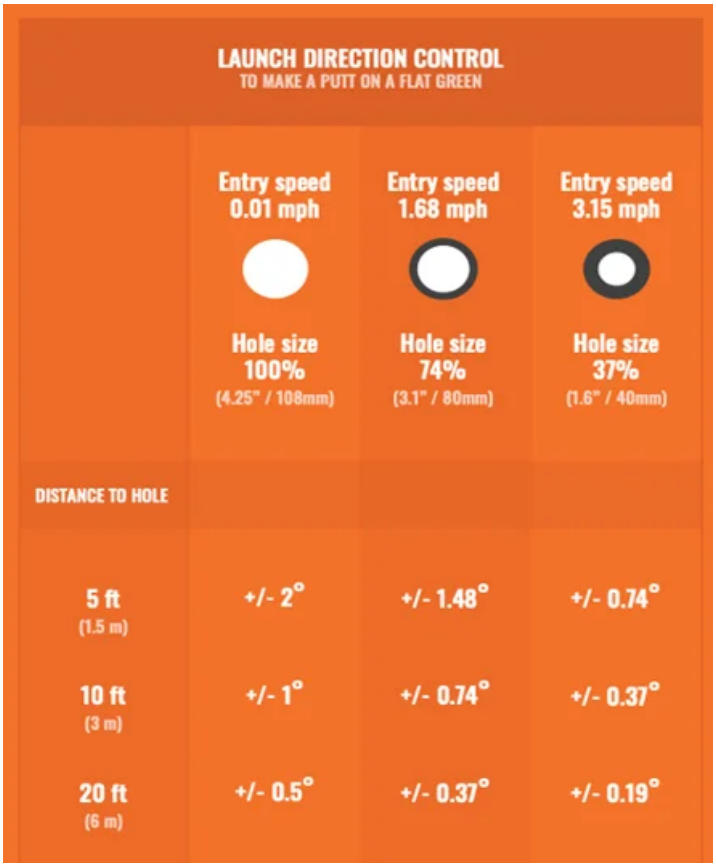

Figure 20. Launch direction requirements for making putt on a flat green[7]

Figure 19 provides a distance and launch direction strategy that defines the launch direction tolerance required for a putt to be made dependent on the size of the whole. For example, the launch direction tolerance for a 5 ft putt is +/- 2 degrees. The 74% hole size is a preferred strategy for most players as it teaches the ability for the putt to have speed that reaches the hole more often without rolling too long. This provides a target that has enough speed to hold the intended line of the putt as there is usually inconsistent break during the final foot of roll due to gravity and green inconsistency. Trackman has determined that launch direction is influenced by a ratio of 13% club path and 87% face angle.

Figure 21. Club path and face angle overlay[7]

Speed control is critical and influences the effective hole size as a PGA player makes 96% of putts from 3 feet and a bogey-golfer makes about 84% from the same distance. It is a common exercise for a golfer to aim to have their putt finish within a 2 ft radius around the hole, but having proper speed control is the most difficult element of that. A

golfer can use the Trackman 4 to track the placement of putts aimed at 10 ft, 20 ft, and 30 ft away to break down the % error, tempo of putting stroke, and stroke length. These parameters will allow a golfer to fine tune their putting stroke and gain a better feel for what physical motions will deliver a putt to an expected distance. Professionals will typically showcase a tempo that is constant (backswing time / forward swing time) regardless of the distance of the putt in order to produce consistent, repeatable results.

Figure 22. Visualization of launch direction, putt break, and straight line to the hole[7]

Total putt evaluation consists of three essential putting skills: green reading, distance control, and directional accuracy. A successful putt will require the golfer to correctly predict the green slope and speed, hit the ball with the right speed for a given putt, and start the ball along the intended aim point within certain tolerances. The evaluation involves a user reading a green, developing a strategy of attack, determining an ideal stop point, and then executing the putting stroke.

REFERENCES

1. Trackman tracking technology - the virtual PGA show 2021, YouTube. (2021). https://www.youtube.com/watch?v=TUGqch7Z2Mc (accessed April 20, 2023).

2. Trackman Golf Performance Software, TrackMan Golf Performance Software. (n.d.). https://www.trackman.com/golf/trackman-4/software (accessed April 20, 2023).

3. N. Heidelberger, How Trackman Golf Systems Are Changing the game, How Trackman Golf Systems Are Changing the Game Golflink.com. (n.d.). https://www.golflink.com/lifestyle/how-trackman-golf-systems-are-changing-game (accessed April 20, 2023).

4. "TrackMan 4." TrackMan, 2021, https://www.trackman.com/golf/trackman-4.

5. PGA Tour selects Trackman Tracking and tracing solution beginning in 2022, PGA TOUR. (2022). https://www.pgatour.com/article/news/latest/2022/02/02/pga-tour-selects-trackman-tracking-tracing-solution-beginning-in-2022 (accessed April 20, 2023).

6. C. Hahn, How trackman 4 determines impact location, TrackMan Golf. (2018). https://blog.trackmangolf.com/how-trackman-4-determines-impact-location/ (accessed April 20, 2023).

7. A. Yeazel, Performance putting – the evaluator, TrackMan Golf. (2020). https://blog.trackmangolf.com/performance-putting-the-evaluator/ (accessed April 20, 2023).

MLB STATCAST

OVERVIEW

In 2015, Major League Baseball (MLB) introduced Statcast - a state-of-the-art technology that collects and analyzes on-the-field data that has never been tracked in the past. Statcast utilized a combination of camera and radar systems from 2015-2019, and now uses Hawk-Eye, a camera system that offers increased tracking ability.[1]

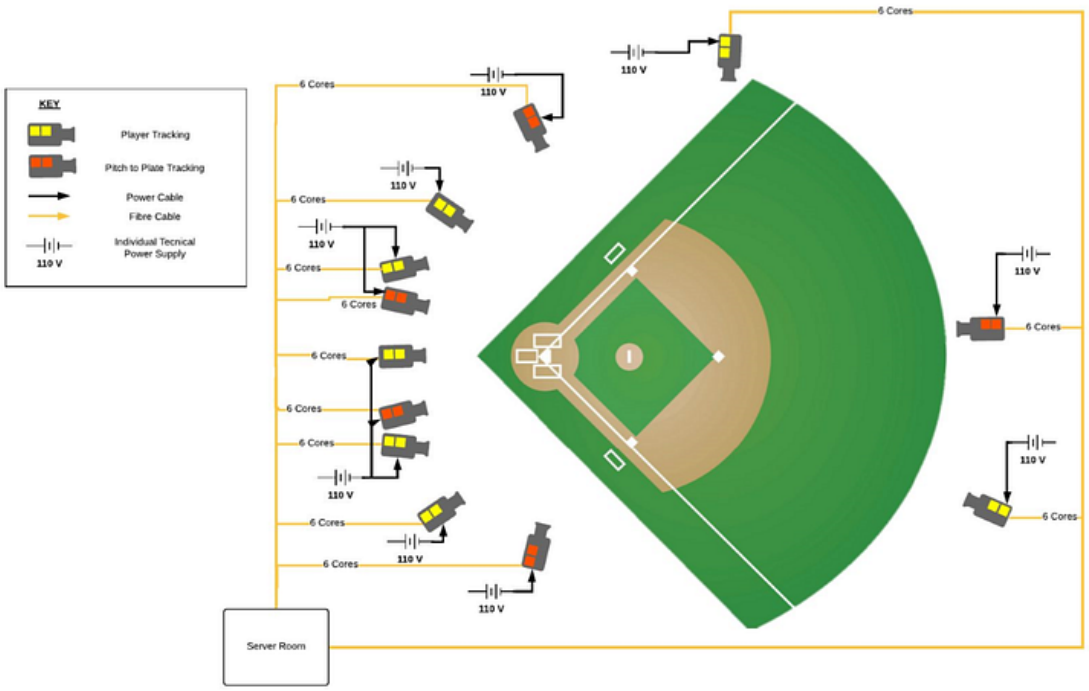

Figure 23. General MLB Statcast ballpark architecture[1]

One of the key additional features is pose tracking, a technology that gets 30 sets of data per second from 18 skeletal points on a player's body. Each stadium is equipped with 12 Hawk-Eye cameras at various locations around the ballpark. 7 of the 12 cameras operate at 50 frames per second and are responsible for tracking players and

batted balls while the remaining 5 cameras have higher frame rates of 100 frames per second and focus on pitch tracking.

The new Trackman phased-array Doppler radar has superseded the Pitch F/X system and is mounted behind home plate. It operates in the X-band and has the added capabilities of measuring a pitch's total spin and batted balls. While this Trackman radar is used to track balls, it is not as useful for tracking players due to players' slower movements causing smaller Doppler shifts. Statcast's ChyronHego system uses two arrays of optical video sensors and stereo vision techniques to track players as three high-resolution camera angles are stitched together.[2]

The metrics gathered by this technology have enabled players to use data and the philosophy behind it to make crucial adjustments to their game. Additionally, front offices are better able to measure the raw performance of players and broadcasters have been able to integrate data into the overall fan experience. Increases in sensor, processor, and storage performance have led to a massive increase in data captured from sporting events. MLB Statcast's combination of Doppler radar and stereoscopic video combine to acquire seven terabytes of data from each game.[3]

MLB teams have been constantly searching for the next big stride in analytics-based models to find a competitive advantage. Oakland A's became the most well-known pioneer of using data as they were able to build a competitive team with their Moneyball approach. This approach is based on the assumption that small-market franchises can

outwin large-market teams with the utilization of analytics to better forecast player performance.[4] MLB Statcast has uncovered several statistics that have become vital to player evaluation in today's sport and will be discussed later in the paper.

Sensor measurements are becoming increasingly prominent in player assessment such as the ability of a catcher to "frame" pitches to increase the probability of a strike call. Some teams were able to determine a way to quantify this skill to gain an advantage on their opponents for a period of time until framing ability was more accurately quantified across the league. These sensor measurements are also being used to better estimate fielding skill as they can calculate the speed and angle of the batted ball to estimate how often a hit ball is fielded, the reaction time, and route efficiency of the fielder.[5]

With more comprehensive data on batter tendencies, defenses are better able to pre-position their team prior to the ball being put into play. A few years after Statcast was implemented into every stadium the MLB saw the frequency of defensive shifts double from 2017 to 2019.[6] In response to the increase in defensive performance and awkward aesthetic of shifts, the MLB implemented a rule change for the 2023 season in efforts to rebalance the entertainment value of the game. The new rule change reads, "At the start of each pitch, teams must have at least two infielders on either side of second base, with all four positioned on the infield dirt. Infielders may not switch positions unless there is a substitution."[6]

SPIN RATE

This is not the first instance that MLB Statcast has had significant influence on rule changes. Prior to 2021, there was a trend of pitchers' spin rates on pitches increasing significantly and it was speculated that foreign substances were the driving factor.[8]

MLB Statcast measures the rotation of the ball in rpms immediately after it is released from the pitcher's hand. A higher spin rate will result in more ball movement as it travels to the plate, which should make it more difficult for the hitter to hit. This is important because pitchers have different pitch types to choose from in order to confuse the batter with balls thrown at different spin rates and velocities. For example, fastballs are thrown with high velocity rather than a high amount of spin since it is better suited for attempting to overpower the batter while a curveball is thrown with a high amount of downward spin that causes the ball to break sharply before reaching the plate. Pitchers that are able to throw pitches at a higher spin rate without sacrificing velocity will be at an advantage over pitchers that throw the same pitch with less movement to confuse batters.[9] A particular advantage that several of the best pitchers have in common is a high velocity fastball (95+ mph) as well as a high spin rate for the pitch type (2400-2800 rpm). Since Statcast was implemented in 2015, spin rate data has demonstrated a trend of higher fastball rates as the figure shows below.

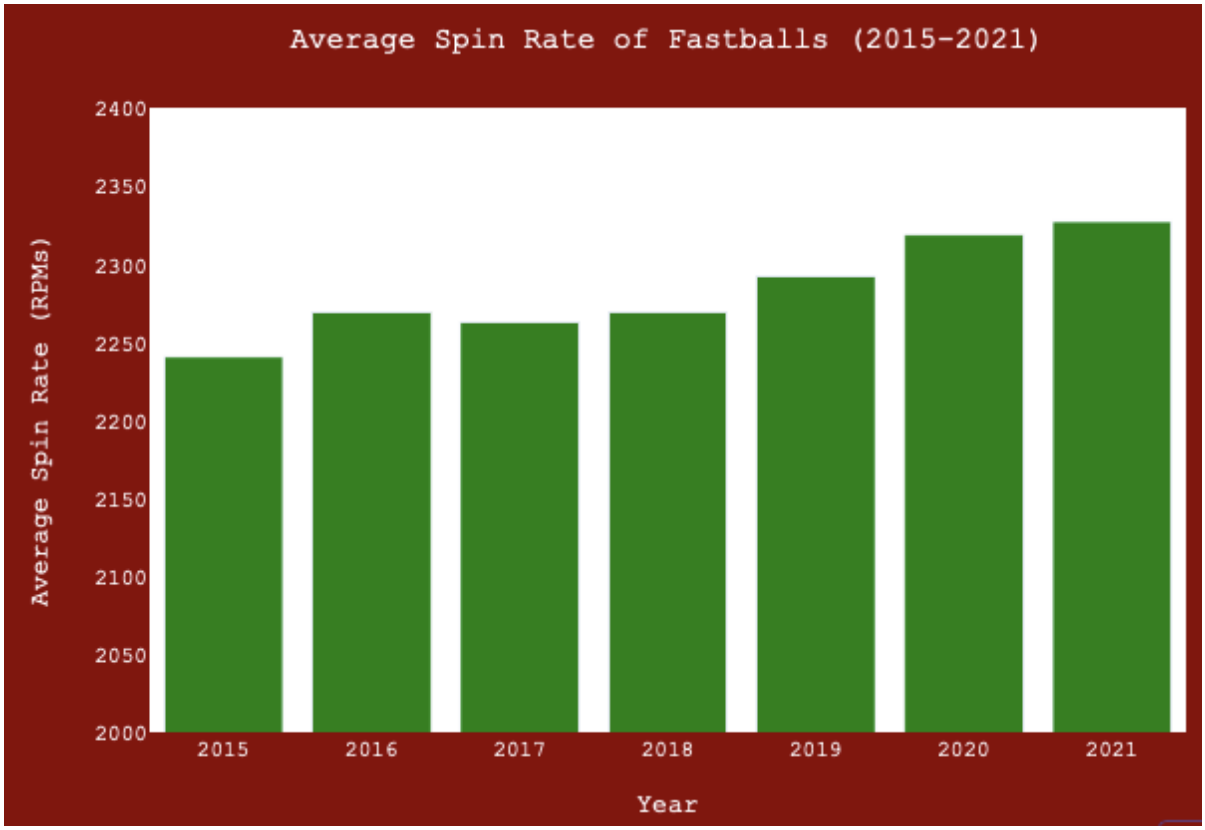

Figure 24. Average fastball spin rate from 2015-2021[10]

Data from the 2018 MLB season shows that batters hit for a 0.279 batting average against fastballs between 93 and 94 mph and 2240-2300 rpm, but hit for a lower batting average, 0.255, against fastballs in the same velocity range with 2540-2600 rpm. The more spin a fastball has, the more it appears to rise and resist gravity and the more swings and misses it causes.

A former top pitcher in the league, Trevor Bauer, is credited for leading the initiative for the MLB to do something about pitchers using illegal foreign substances to increase their spin rates. He estimated that 70% of pitchers in the league were using a foreign

substance and has sarcastically responded to data analysts looking into the same trend on Twitter.[11]

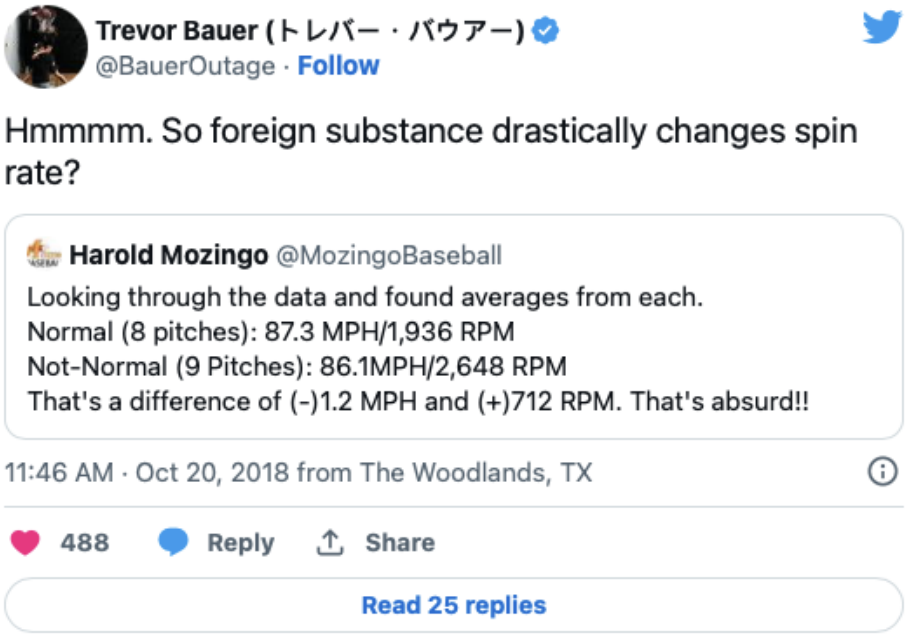

Figure 25. Trevor Bauer tweet regarding spin rate controversy[11]

When the MLB was complacent about acting on the foreign substance issue in its game, Bauer decided that he would partake in the movement as well. He said, “There is a problem in baseball right now that has to do with sticky substances and spin rates. We know how it affects spin rate and we know how spin rate affects outcomes and pitches and movements that have a big difference in a game, a season and each individual player’s career… The people who choose not to do it are at a competitive disadvantage.”[11]

A physics professor and MLB consultant, Alan Nathan, argues that “It’s probably pretty hard to change that [fastball spin] ratio for an individual,” Nathan said of naturally changing spin rate. “I can see that you could do it for a curveball because a curveball involves some technique whereas a fastball is pure power. There is no finesse.”[9]

In June 2021, the MLB announced new midseason rule enforcement changes in response to the growing issue of foreign substances. At this point in the 2021 season, hits were at record lows, strikeouts were at record highs, and more than a typical season’s worth of no-hitters were thrown just seven weeks into the season.[12] In the past, the league has not strictly enforced rules relevant to the topic and players had significant leeway as long as the tampering was not blatant.

Rule 3.01 states, “no player shall intentionally discolor or damage the ball by rubbing it with soil, rosin, paraffin, licorice, sand-paper, emery-paper or other foreign substance.” Similarly, Rule 6.02(c), an expansion of Rule 3.01, explains that pitchers may not “apply a foreign substance of any kind to the ball;" "deface the ball in any manner;" throw a shine ball, spit ball, mud ball, or emery ball; "have on his person, or in his possession, any foreign substance;" or "attach anything to his hand, any finger or either wrist (e.g., Band-Aid, tape, Super Glue, bracelet, etc.)."[7]

The enforcement of the Rule 3.01 and Rule 6.02(c) will now require:

- periodic substance checks throughout the game for both starting pitchers and relief pitchers
- checks any time a ball feels “unusually sticky” or when an umpire observes a pitcher going the his glove hat, belt or any other part of his uniform or body to retrieve or apply what may be a foreign substance
- catchers being subject to inspections

Consequences for pitchers who violate these rules will be suspended 10 days without pay if caught and the team will not be able to replace the suspended player on their 26-man active roster. Additionally, if a player refuses to cooperate with the umpire conducting an examination, the player will be presumed guilty, ejected from the game, and suspended.[7]

A New York Times article explored MLB Statcast data regarding spin rates before and after the increased scrutiny surrounding foreign substance use in the 2021 season. The league had announced on June 3 that the issue will be dealt with directly and a steep drop in spin rates was seen immediately after. After the league announced its increased enforcement plan regarding Rule 3.01 and Rule 6.02(c), the spin rate decline began to level off. After June 15, 2021, walks had increased for the first time in decades, the strikeout rate had dropped to 23.0% from 24.2%, and batters saw the biggest increase in on-base percentage since at least 1990.[13]

The New York Times examined data from every fastball from 2017 to 2021, about 1.7 million pitches in all, and compared the change in spin rates in previous seasons with the rates in 2021.Of the 131 pitchers that had thrown at least 150 fastballs from June 15 to the publishing date of the article, fastball spin rates fell for 103 of them. This is a significant insight because a pitcher's spin rate does not typically change much over the course of the season.[13]

MLB commissioner commented on the effects on the implemented rule changes and said, "Enforcing our rules is really important — they're on the books, they should be enforced," and called the changes in play "very promising." In contrast, Yankees pitcher Gerrit Cole complained that "There was no real legislation on the customs and practices that were going on," and that it has been challenging for players to adjust quickly.[13]

LAUNCH ANGLE

MLB Statcast has led to drastic changes in hitting philosophies across the league as the data is suggesting that batters should aim to hit the ball at a launch angle between 25-35 degrees at an exit velocity of 95 mph or greater in order to hit more home runs. The launch angle is "the vertical angle at which the ball leaves a player's bat after being struck" and exit velocity corresponds to the velocity "with which a struck ball leaves the hitter's bat.[14] Higher exit velocities are associated with better contact, increasing the likelihood of a hit." For decades, baseball coaches pounded the hitting philosophy of swinging down on the ball, and it turns out that they were wrong all along.[15]

The Oakland A's were one of the first teams that initiated the "flyball movement" as their 2012 and 2013 teams led the league in fly balls, and they won the American League West division both years. The same organization that was applauded for their clever use of baseball analytics to maximize the value of their small payroll to compete with larger market teams is credited with first identifying and exploiting the market inefficiency of flyball hitters.

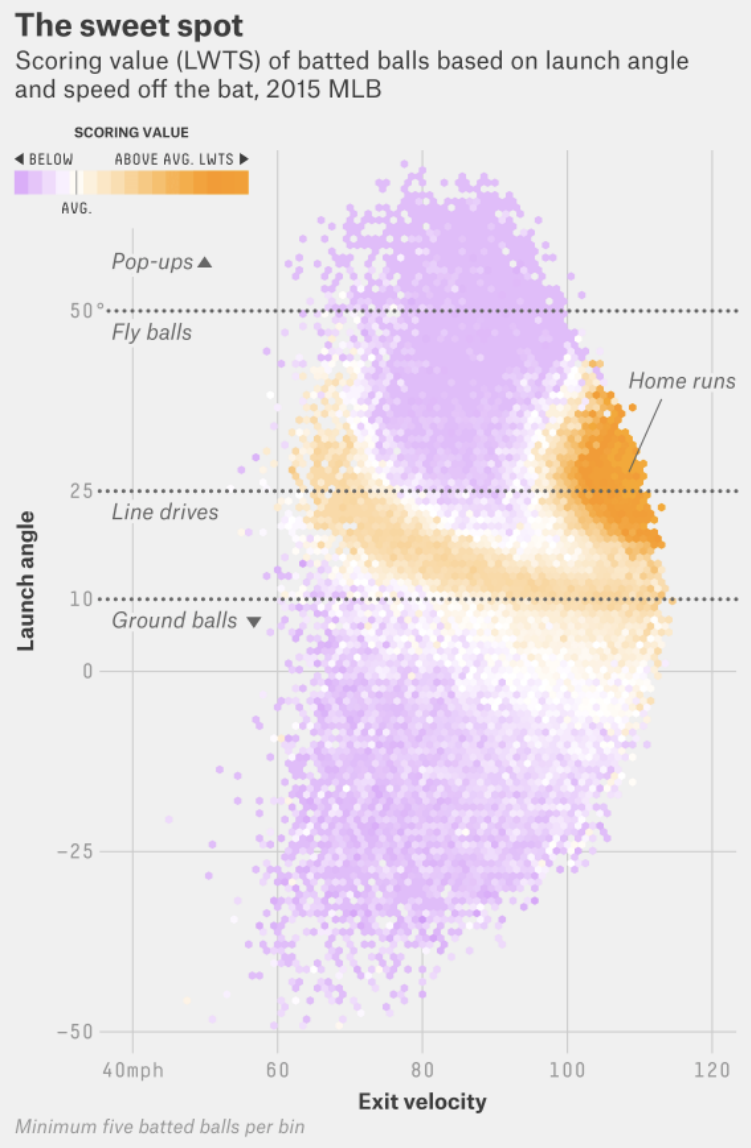

Figure 26. Scoring value of batted balls in 2015 based on launch angle and exit velocity[17]

Some players were eager to adopt this new philosophy quickly after Statcast was implemented in 2015. For example, former 2015 American League Most Valuable Player, Josh Donaldson said, “Ground Balls are outs. If you see me hit a ground ball, even if it’s a hit, I can tell you: It was an accident.”[17]

However, some players were reluctant to this trend as they have years of muscle memory and training of trying to hit the ball hard and down. Chase Headley, former Padres third baseman, recalls that his swing used to produce more launch angle, but his team had suggested that the team’s hitters keep the ball out of the air due to their ballpark’s dimensions. Years later in the Statcast era, Headley’s new team, the New York Yankees, urged him to resist his old coaching. He remembers that he couldn’t “help but kick himself for not resisting the Padres’ efforts to turn him into a ground ball machine.”[5]

The logic behind the claim is that slugging percentage, the total number of bases a player records per at-bat, is driven by balls hit in the air. In 2016, batters hit .239 with a .258 slugging percentage on ground balls vs. .241 and .715, on fly balls. This large discrepancy between slugging percentages is attributable to home runs as ground balls obviously produced zero, while fly balls produced 5,422.[5]

An article published by the Washington Post highlights that the average launch angle in the MLB was 10.5 degrees and that average rose to 11.5 degrees in 2016, and 12.8 degrees as of May 21 in the 2017 season. This has proved to be a massive development in modern baseball as the rate teams have implemented defensive shifts was 10x higher in 2017 than just six years prior since teams had access to information about hitter tendencies. As a result, hitters aimed to hit the ball where defenders could not play, the bleachers, and this led to an overall increase in home runs. The 2016 season featured 5,610 home runs (a 14% increase from 2015) and the most since the 2000 season, which is considered to be the peak of performance enhancing drug use across the sport.[16]

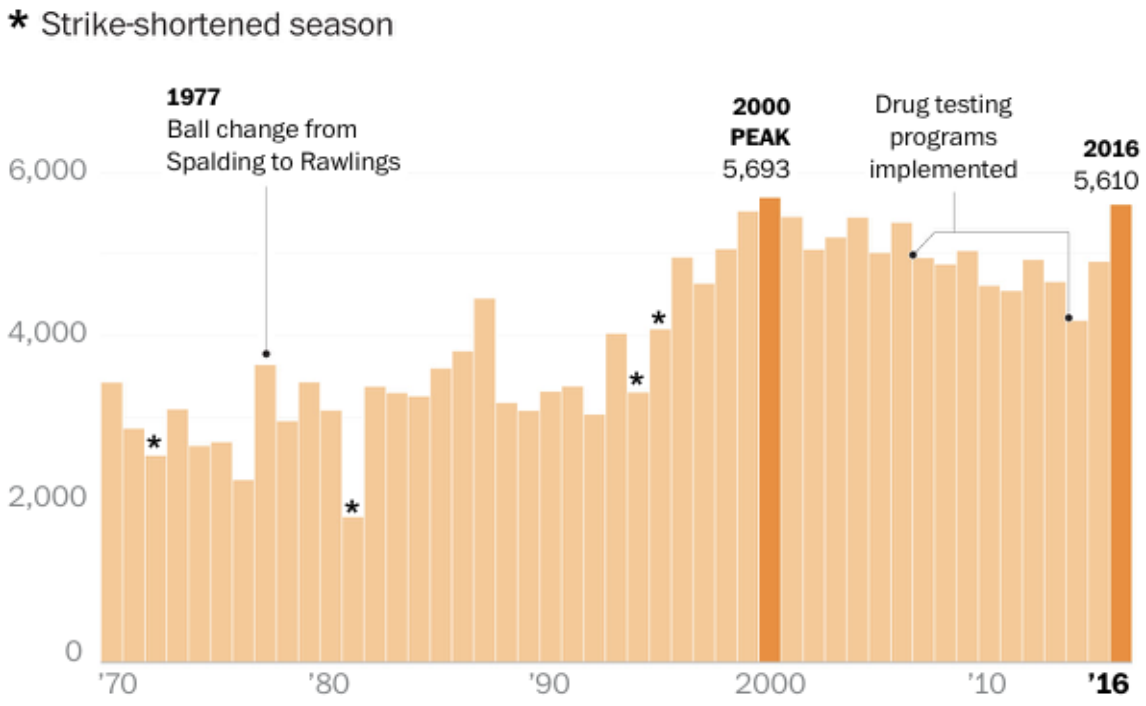

Figure 27. Total home runs in a season from 1970-2016[16]

A consequence of hitters swinging for the fences is that games have slowed in pace as hitters have become more willing to swing and miss, forcing pitchers to throw more pitches. Also, pitchers have taken longer between pitches to focus on not throwing any mistake pitches. Forty years ago, the average MLB game took 2 hours and 33 minutes and that number gradually increased to 3 hours and 10 minutes as of 2021. The sport has become less popular with sports fans and MLB commissioner Rob Manfred has noted the change of hitting philosophies as one of the reasons for baseball's slowing pace of play.[18]

New to the 2023 MLB season are several rule changes designed to shorten games. After experimentation in over 8,000 Minor League games, the Joint Competition Committee voted in favor of a pitch timer. There are now various time limits, ranging from 15 to 30 seconds, for the pitcher to begin their motion to deliver the pitch and batters to be in hitting position. As a consequence, an automatic ball or strike is called depending on who is at fault for the violation. As of April 10, 2023, the average game time is down 31 minutes and on track to be the lowest since 1984 and two thirds of pitch clock penalties have been imposed on pitchers. This is one of the three new rules that the MLB hopes will have a lasting impact on shortening games, increasing offense, and creating a more exciting product for the sport's fans.[7]

REFERENCES

1. Jedlovec, Ben. "Introducing Statcast 2020: Hawk-Eye and Google Cloud." MLB Technology Blog, 17 Feb. 2020, https://technology.mlblogs.com/introducing-statcast-2020-hawk-eye-and-google-cloud-a5f5c20321b8.

2. "MLB Teams Prepare for 2023 Season with New Technology Updates." Sports Business Journal, 27 Mar. 2023, https://www.sportsbusinessjournal.com/Journal/Issues/2023/03/27/Technology/mlb-2023-season-technology-updates.aspx.

3. Healey G. Combining Radar and Optical Sensor Data to Measure Player Value in Baseball. Sensors (Basel). 2020 Dec 24;21(1):64. doi: 10.3390/s21010064. PMID: 33374299; PMCID: PMC7796355.

4. Bechtold, Taylor. "State of Analytics: How the Movement Has Forever Changed Baseball, for Better or Worse." Stats Perform, 11 Sept. 2019, https://www.statsperform.com/resource/state-of-analytics-how-the-movement-has-forever-changed-baseball-for-better-or-worse/.

5. Saunders, Patrick. “How Statcast Is Changing the Way MLB Teams Think About Defense.” The Denver Post, 2 June 2017, https://www.denverpost.com/2017/06/02/statcast-launch-angle/.

6. Verducci, Tom. "Banning Infield Shifts Would Have a Major Impact on MLB." Sports Illustrated, 21 Nov. 2022, https://www.si.com/mlb/2022/11/21/banning-infield-shifts-impact.

7. Castrovince, Anthony. "MLB Announces Rule Changes for 2023 Season." MLB.com, 8 Mar. 2023, https://www.mlb.com/news/mlb-2023-rule-changes-pitch-timer-larger-bases-shifts

8. Cheng, Eric. “Analyzing Baseball's Spin Rate Revolution.” Towards Data Science, 16 May 2018, https://etsc9287.medium.com/analyzing-baseballs-spin-rate-revolution-901e022ba60d.

9. Longenhagen, Eric, and Kiley McDaniel. “Baseball's Top Staffs Have Come Around on the High-Spin Fastball.” FiveThirtyEight, 16 June 2021, https://fivethirtyeight.com/features/baseballs-top-staffs-have-come-around-on-the-high-spin-fastball/.

10. Schacht, Ethan. "Analyzing Baseball's Spin Rate Revolution." Medium, 26 Oct. 2021, https://etsc9287.medium.com/analyzing-baseballs-spin-rate-revolution-901e022ba60d.

11. Boswell, Thomas. "Major League Baseball’s foreign substance crackdown is a mess." Washington Post, 8 June 2021, https://www.washingtonpost.com/sports/2021/06/08/mlb-baseball-doctoring-enforcement/.

12. Bialik, Carl, and Kevin Quealy. "What Changed in MLB After It Tried to Stop Pitchers' Sticky-Fingered Ways." The New York Times, 19 July 2021, https://www.nytimes.com/interactive/2021/07/19/upshot/major-league-baseball-spin-rate-shift.html.

13. Bialik, Carl, and Rob Arthur. “As Baseball Cracks Down on Pitchers, Spin Rates Are Already Dropping.” The New York Times, 19 July 2021, https://www.nytimes.com/interactive/2021/07/19/upshot/major-league-baseball-spin-rate-shift.html.

14. "Launch Angle." MLB.com, n.d., https://www.mlb.com/glossary/statcast/launch-angle#:%7E:text=Launch%20Angle%20represents%20the%20vertical,ball%3A%20Less%20than%2010%20degrees.

15. Lemire, Joe. "The Statcast Revolution: How MLB's Latest Tech Is Wowing Fans, Scaring Pitchers and Making GMs Salivate." Vocativ, 9 May 2017, https://www.vocativ.com/434373/statcast-mlb-home-run-surge/index.html.

16. Wagner, James. “The Launch Angle Revolution Is Real and MLB Must Adapt or Die.” The Washington Post, WP Company, 14 Apr. 2016, https://www.washingtonpost.com/graphics/sports/mlb-launch-angles-story/.

17. Sheinin, Dave. “Fly Ball Revolution: How the MLB Home Run Surge Is Altering the Sport.” The Washington Post, WP Company, 14 June 2017, www.washingtonpost.com/graphics/sports/mlb-launch-angles-story/.

18. Passan, Jeff. “MLB's Game in 31 Minutes: Inside the Plan to Speed Up Baseball's Pace.” ESPN, 12 Aug. 2021, https://www.espn.com/mlb/story/_/id/36149872/mlb-game-s-31-minutes-rule-changes.

CONCLUSION

Radar has seen significant technological improvement to become a versatile and powerful tool since its inception in the late 19th century. It has become vital to sports tracking, which employs Doppler radar to track the motion of targets such as golf balls and baseballs. Radar technology has changed the way that we understand and analyze performance as Trackman has provided players detailed data about their swings, ball flight, and clubhead speed. It has become a tool for monitoring nominal pitcher spin rate patterns that can alert league officials of potential illegal foreign substance use to give the pitcher a stronger grip. Technological advancements in radar will continue to push the boundaries of what is possible and drive innovation across a wide range of industries.